Circulation: Arrhythmia and Electrophysiology

ORIGINAL ARTICLE

NPR-C (Natriuretic Peptide Receptor-C) Modulates the Progression of Angiotensin II–Mediated Atrial Fibrillation and Atrial Remodeling in Mice

Hailey J. Jansen, PhD*
Martin Mackasey, BSc*
Motahareh Moghtadaei, PhD
Yingjie Liu, PhD
Jaspreet Kaur, PhD
Emmanuel E. Egom, MD, PhD
Jari M. Tuomi, MD, PhD
Sara A. Rafferty, MSc
Adam W. Kirkby, MSc
Robert A. Rose, PhD

BACKGROUND: Atrial fibrillation (AF) commonly occurs in hypertension and in association with elevated Ang II (angiotensin II) levels. The specific mechanisms underlying Ang II–mediated AF are unclear, and interventions to prevent the effects of Ang II are lacking. NPs (natriuretic peptides), which elicit their effects through specific NP receptors, including NPR-C (natriuretic peptide receptor-C), are cardioprotective hormones that affect cardiac structure and function.

METHODS: This study used wild-type and NPR-C knockout (NPR-C$^{-/-}$) mice to investigate the effects of Ang II (3 mg/kg per day for 3 weeks) on AF susceptibility and atrial function using in vivo electrophysiology, high-resolution optical mapping, patch clamping, and molecular biology. In some experiments, wild-type mice were cotreated with Ang II and the NPR-C agonist cANF (0.07–0.14 mg/kg per day) for 3 weeks.

RESULTS: In wild-type mice, Ang II increased susceptibility to AF in association with a prolongation of P-wave duration, increased atrial refractory period, and slowed atrial conduction. These effects were exacerbated in Ang II–treated NPR-C$^{-/-}$ mice. Ang II prolonged action potential duration and reduced action potential upstroke velocity (V_{max}). These effects were greater in left atrial myocytes from Ang II–treated NPR-C$^{-/-}$ mice. Ang II also increased fibrosis in both atria in wild-type mice, whereas Ang II–treated NPR-C$^{-/-}$ mice exhibited substantially higher fibrosis throughout the atria. Fibrotic responses were associated with changes in expression of profibrotic genes, including *TGFβ* and *TIMP1*. Cotreating wild-type mice with Ang II and the NPR-C agonist cANF dose dependently reduced AF inducibility by preventing some of the Ang II–induced changes in atrial myocyte electrophysiology and preventing fibrosis throughout the atria.

CONCLUSIONS: NPR-C may represent a new target for the prevention of Ang II–induced AF via protective effects on atrial electrical and structural remodeling.

VISUAL OVERVIEW: A visual overview is available for this article.

*Dr Jansen and M. Mackasey contributed equally to this work co-first authors.

Key Words: action potentials ■ extracellular matrix ■ fibrosis ■ ion channels ■ natriuretic peptides

https://www.ahajournals.org/journal/circep

WHAT IS KNOWN?

- Atrial fibrillation is prevalent in hypertension and in the setting of elevated Ang II (angiotensin II) and can occur in association with electrical and structural remodeling in the atria.
- Natriuretic peptides are cardioprotective hormones that elicit their effects, in part, through NPR-C (natriuretic peptide receptor-C).

WHAT THE STUDY ADDS?

- Ang II treatment in wild-type mice increased susceptibility to induced atrial fibrillation and slowed atrial conduction in association with alterations in atrial myocyte electrophysiology and increased atrial fibrosis.
- The effects of Ang II on atrial arrhythmogenesis and electrophysiology were exacerbated in mice lacking NPR-C, whereas the treatment of wild-type mice with an NPR-C activator protected against the effects of Ang II.
- The NPR-C receptor may represent a new target for the prevention of Ang II–induced atrial fibrillation.

Atrial fibrillation (AF)—the most common sustained cardiac arrhythmia—is a major clinical challenge because it increases morbidity and mortality due to complications such as stroke and heart failure.[1–3] Hypertension, which can be associated with increased levels of Ang II (angiotensin II), is a risk factor for AF.[2] Furthermore, pathological Ang II signaling has been directly implicated in AF.[2,4–6] Despite these links, the mechanisms by which Ang II and hypertension lead to AF are not well understood, and interventions to modify the development of Ang II–mediated AF are lacking.

AF can occur in association with electrical remodeling (ie, changes in ion channel function) and structural remodeling (ie, fibrosis) of the atria and requires both a trigger to initiate AF and a proarrhythmic substrate that sustains the arrhythmia.[1,2] Electrical remodeling and fibrosis have each been shown to contribute to AF initiation and maintenance.[2,3]

Electrical remodeling can occur because of alterations in action potential (AP) morphology that can result in the initiation or maintenance of AF. The sodium current (I_{Na}, carried by $Na_V1.5$ channels) is responsible for the AP upstroke velocity and plays a key role in electrical impulse propagation across the myocardium and, therefore, atrial conduction velocity (CV).[7,8] AP duration is determined by the balance between the inward L-type calcium current ($I_{Ca,L}$, carried by $Ca_V1.2$ and $Ca_V1.3$ channels)[9] and several repolarizing potassium (K^+) currents, including the transient outward K^+ current (I_{to}, carried by $K_V4.2$ and $K_V4.3$ channels), the ultrarapid delayed rectifier K^+ channel (I_{Kur}, carried by $K_V1.5$ channels), and a steady-state K^+ current (I_{Kss}, carried by $K_V2.1$ channels).[7,10] In some species, the rapid delayed rectifier K^+ current (I_{Kr}) and the slowly activating delayed rectifier K^+ current (I_{Ks}) also contribute to AP repolarization.[10] Alterations in these ionic currents can prolong AP repolarization, which can promote the development of early afterdepolarizations that can serve as triggers for AF.[2,11]

Enhanced cardiac fibrosis is a key feature of structural remodeling that can create local conduction disturbances and conduction block, which may promote reentry.[3,6,12,13] Specifically, increased levels of fibrosis in the atria can disrupt myocyte connectivity and lead to slow conduction, thereby shortening the wavelength for reentry and favoring the maintenance of AF. Increased interstitial fibrosis can occur in a number of ways including in association with increases in collagen expression and deposition, as well as changes in extracellular matrix remodeling by MMPs (matrix metalloproteinases) and TIMPs (tissue inhibitors of metalloproteinases).[3,14,15]

NPs (natriuretic peptides) are a family of cardioprotective hormones that elicit their biological effects by binding to NP receptors denoted NPR (NP receptor)-A, NPR-B, and NPR-C.[16–19] NPR-C is the most highly expressed receptor in the atrial myocardium[20,21] but also the least studied NPR. NPs are critical regulators of atrial structure and electrophysiology, and some of these effects are mediated through NPR-C.[17,19,22] Acute activation of NPR-C can modulate ion channel function in the heart, including in the atria.[17] NPs are also known to have antifibrotic effects that can be mediated, in part, by NPR-C.[19] We have recently demonstrated that NPR-C–deficient ($NPR\text{-}C^{-/-}$) mice have an increased susceptibility to AF in conjunction with slowed atrial conduction.[20] These effects were primarily because of enhanced atrial fibrosis in $NPR\text{-}C^{-/-}$ mice. This suggests that NPR-C may play a protective role against the development of AF; however, the role of NPR-C in modulating atrial structure and electrophysiology in Ang II–mediated AF is unknown.

In the present study, we have used a mouse model of hypertension caused by chronic Ang II treatment and investigated the role of NPR-C in the progression of Ang II–mediated atrial dysfunction and arrhythmogenesis. Our study demonstrates a critical role for NPR-C in protecting against Ang II–mediated AF through effects on structural and electrical remodeling.

METHODS

An expanded methods section is provided in Materials in the Data Supplement. The data, analytic methods, and study materials will be made available to other researchers for the purpose of reproducing the results or replicating the procedures.

Mice

This study utilized male wild-type (C57BL/6) or NPR-C$^{-/-}$ (strain B6;C-*Npr3*^{tm1Gjj}/J; Jackson Laboratory) mice between the ages of 10 and 15 weeks. NPR-C$^{-/-}$ mice were backcrossed into the C57Bl/6 line and bred locally. Mice were implanted with a subcutaneous miniosmotic pump (Alzet) to allow for continuous delivery of saline, Ang II (3 mg/kg per day; Bachem), or Ang II with cANF ([des(Gln$_{18}$, Ser$_{19}$, Gly$_{20}$, Leu$_{21}$, Gly$_{22}$)ANP$_{4-23}$-NH$_2$] a selective NPR-C agonist[19,23,24]; 0.07 or 0.14 mg/kg per day; Bachem). In the majority of cases, Ang II was delivered for 3 weeks, except for some gene expression studies, which were conducted after 3 days and 3 weeks of Ang II treatment. When used, cANF was delivered for 3 weeks along with Ang II. Animal protocols were approved by the University of Calgary Animal Care Committee and the Dalhousie University Committee for Laboratory Animals and were in accordance with the Canadian Council on Animal Care.

Blood Pressure

Blood pressure was measured in conscious, restrained mice using a tail-cuff apparatus (IITC Life Sci). Baseline measurements were taken before mini osmotic pump implantation, and end point measurements were obtained at the 3-week time point.

In Vivo Electrophysiology and Arrhythmia Studies

Surface ECGs were recorded in anaesthetized mice (2% isoflurane inhalation) using 30 gauge subdermal needle electrodes (Grass Technologies) placed in a lead II conformation. To perform intracardiac programed electrical stimulation, a 1.2F octopolar electrophysiology catheter (Transonic) was inserted into the right heart via an incision made in the jugular vein. Correct catheter placement was achieved by obtaining a predominantly atrial signal in the proximal lead and a sole ventricular signal in the distal lead. Rapid burst pacing of the right atrium was used to induce AF in anaesthetized mice, as we have done previously.[20,25] AF was defined as a rapid and irregular atrial rhythm as indicated by a fibrillatory baseline in association with irregular R-R intervals that persisted for at least 1 s on the surface ECG. AF duration was categorized into 3 groups: <5 s (brief), 5–30 s (nonsustained), or >30s (sustained) to determine the severity of AF when induced.[25,26] Atrial effective refractory period (AERP) and atrioventricular node effective refractory period were determined using a S1-S2 protocol, as described in the Data Supplement. Body temperature was maintained at 37°C using a heating pad. Additional details are provided in Materials in the Data Supplement.

High-Resolution Optical Mapping

High-resolution optical mapping was used to investigate activation patterns, electrical conduction, and optical AP duration in isolated atrial preparations as we have done previously.[20,27–30] Briefly, atrial preparations were immobilized using blebbistatin (10 μmol/L) and superfused with the voltage-sensitive dye Di-4-ANEPPS (10 μmol/L). Changes in fluorescence were captured using a high-speed EMCCD camera at ≈900 frames per second using a spatial resolution of 67×67 μm per pixel. Data were analyzed in Matlab using custom designed software. Additional details are provided in Materials in the Data Supplement.

Patch Clamping of Isolated Atrial Myocytes

Right and left atrial myocytes were isolated and used to record stimulated APs, I_K, and I_{Na} using the perforated or whole-cell configuration of the patch-clamp technique as we have described previously.[21,31] Additional details are provided in Materials in the Data Supplement.

Western Blotting

Right and left atrial appendages were used to measure the protein expression of PKC (protein kinase C)-α, NPR-A, NPR-B, NPR-C, K_V4.2, K_V4.3, KChIP2, and K_V1.5. GAPDH was used as a loading control. Experimental details are provided in Materials in the Data Supplement.

Quantitative Polymerase Chain Reaction

Quantitative polymerase chain reaction experiments were performed as we have described previously[20,25] using primers to measure *Col1a2* (collagen type I), *Col3a1* (collagen type III), *TGFβ* (transforming growth factor β), *Timp1-4*, *Npr1* (NPR-A), *Npr2* (NPR-B), and *Npr3* (NPR-C) mRNA expression in the right and left atrial appendage. *GAPDH* and *β-actin* were used as reference genes. Additional details and primer sequences are provided in Materials in the Data Supplement.

Collagen Staining

Interstitial collagen was assessed using Picrosirius red (collagen) and fast green (myocardium) staining of paraffin-embedded sections (3 μm) through the right and left atrial appendage. The level of fibrosis was quantified using ImageJ software as described previously.[20,25]

Statistical Analysis

Data are expressed as means±SEM. Statistical analysis was performed using Fisher exact test, Student *t* test, 1-way ANOVA with Tukey post hoc test, 2-way ANOVA with Tukey post hoc test, or 2-way repeated measures ANOVA with Tukey post hoc test as indicated in the figure legends. P <0.05 was considered statistically significant.

RESULTS

Effects of Ang II on AF and Atrial Electrophysiology in Wild-Type and NPR-C$^{-/-}$ Mice

Assessment of systolic blood pressure after 3 weeks of Ang II treatment in wild-type and NPR-C$^{-/-}$ mice demonstrates that Ang II increased (P<0.05) systolic blood pressure in both genotypes compared with saline-treated controls (Figure I in the Data Supplement). Further-

more, the increase in systolic blood pressure was not different (P=0.267) between wild-type and NPR-C$^{-/-}$ mice (Figure I in the Data Supplement).

Susceptibility to AF in wild-type and NPR-C$^{-/-}$ mice after Ang II treatment was assessed in vivo by burst pacing in the right atrium (Figure 1A). These data demonstrate that Ang II increased (P<0.05) the inducibility of AF in wild-type and NPR-C$^{-/-}$ mice and that NPR-C$^{-/-}$ mice treated with Ang II displayed more AF (P<0.05) than Ang II–treated wild-type mice (Figure 1B). AF duration was brief (ie, <5 s before spontaneous reversion back to sinus rhythm) in the 2 saline-treated wild-type mice that were induced into AF (Figure 1C; Table I in the Data Supplement). In contrast, AF was more likely to be longer in duration in Ang II–treated wild-type mice. Strikingly, NPR-C$^{-/-}$ mice treated with Ang II displayed the longest lasting AF, which was >30 s in 30% of cases (Figure 1C; Table I in the Data Supplement).

Measurements of P-wave duration (Figure 1D) and AERP (Figure 1E) demonstrate changes in atrial electrophysiology after Ang II treatment (Table II in the Data Supplement). Specifically, P-wave duration was prolonged (P<0.05) after Ang II treatment in wild-type mice and further increased (P<0.05) in NPR-C$^{-/-}$ mice treated with Ang II. Similarly, Ang II treatment caused an increase in AERP in wild-type mice and a greater increase (P<0.05) in Ang II–treated NPR-C$^{-/-}$ mice.

Conduction in the atria was also assessed in isolated atrial preparations using high-resolution optical mapping. Representative activation maps demonstrate that conduction time across the atria was progressively slowed after Ang II treatment in wild-type and NPR-C$^{-/-}$ mice (Figure 1F). Consistent with our recent findings,[30,32] cycle length was increased (P<0.05) after Ang II treatment (Figure 1G). Furthermore, cycle length was prolonged to a greater extent (P<0.05) in Ang II–treated NPR-C$^{-/-}$ mice (Figure 1G). Quantification of right and left atrial CV during sinus rhythm revealed that Ang II decreased (P<0.05) CV in both atria in wild-type mice and that right and left atrial CV was reduced to a greater extent (P<0.05) in Ang II–treated NPR-C$^{-/-}$ mice (Figure 1H and 1I). Because CV can be affected by beating rate, we also quantified atrial CV in atrial preparations paced at a fixed cycle length of 125 ms (Figure II in the Data Supplement). These data demonstrate that the reductions in right and left atrial CV in Ang II–treated wild-type and NPR-C$^{-/-}$ mice were similar during fixed pacing and in sinus rhythm.

In addition, we measured right and left atrial optical AP duration (APD) from our optical mapping studies (Figure IIIA in the Data Supplement). These data demonstrate that Ang II treatment resulted in similar increases (P<0.05) in APD_{50} (Figure IIIC in the Data Supplement) and APD_{70} (Figure IIID in the Data Supplement) in wild-type and NPR-C$^{-/-}$ mice in the right atrium. Ang II also increased (P<0.05) APD_{50} (Figure IIIE in the Data Supplement) and APD_{70} (Figure IIIF in the Data Supplement) in the left atrium in wild-type and NPR-C$^{-/-}$ mice; however, these increases were larger (P<0.05) in NPR-C$^{-/-}$ mice. The effects of Ang II on atrial AP morphology were investigated in further detail in isolated myocytes as described below. Collectively, these data demonstrate that absence of NPR-C results in more severe atrial arrhythmogenesis and larger impairments in atrial electrophysiology, despite similar increases in systolic blood pressure in Ang II–treated wild-type and NPR-C$^{-/-}$ mice.

Effects of Ang II on Atrial Myocyte Electrophysiology in Wild-Type and NPR-C$^{-/-}$ Mice

AP morphology was measured in right and left atrial myocytes isolated from wild-type and NPR-C$^{-/-}$ mice treated with saline or Ang II (Figure 2A and 2B). Ang II did not increase (P=0.772) cell capacitance in right atrial myocytes from wild-type mice; however, cell capacitance was increased (P<0.05) in right atrial myocytes from Ang II–treated NPR-C$^{-/-}$ mice (Figure IVA in the Data Supplement). In left atrial myocytes, cell capacitance was increased (P<0.05) in wild-type and NPR-C$^{-/-}$ mice after Ang II treatment (Figure IVB in the Data Supplement).

In right atrial myocytes, Ang II had no effect (P=0.399) on AP V_{max} in wild-type or NPR-C$^{-/-}$ mice (Figure 2C); however, Ang II increased (P<0.05) right atrial APD_{20} (Figure 2D), APD_{50} (Figure 2E), and APD_{90} (Figure 2F) in wild-type and NPR-C$^{-/-}$ mice. In right atrial myocytes there was no difference (P=0.393) in the magnitude of the effect of Ang II on APD between wild-type and NPR-C$^{-/-}$ mice (Table III in the Data Supplement). In contrast, Ang II caused a reduction in AP V_{max} in left atrial myocytes from wild-type mice and an even greater reduction (P<0.05) in V_{max} in left atrial myocytes from Ang II–treated NPR-C$^{-/-}$ mice (Figure 2G). Furthermore, Ang II increased (P<0.05) APD in left atrial myocytes from wild-type and NPR-C$^{-/-}$ mice with the increases being larger (P<0.05) in NPR-C$^{-/-}$ mice (Figure 2H through 2J; Table IV in the Data Supplement). Thus, Ang II had distinct effects on atrial AP morphology that depended on the presence or absence of NPR-C, as well as which atrium was investigated.

Because Ang II reduced AP V_{max} only in the left atrium, we measured left atrial I_{Na} in wild-type and NPR-C$^{-/-}$ mice after Ang II or saline treatment (Figure 3A). I_{Na} IV curves demonstrate that Ang II treatment reduced (P<0.05) I_{Na} density in wild-type (Figure 3B) and NPR-C$^{-/-}$ (Figure 3C) mice in association with reductions (P<0.05) in I_{Na} conductance as measured from steady-state activation curves (Figure 3D and 3E). Analysis of I_{Na} activation kinetics demonstrates that G_{max} was reduced (P<0.05) in Ang II–treated left atrial myocytes from wild-type and NPR-C$^{-/-}$ mice but that the reduction in

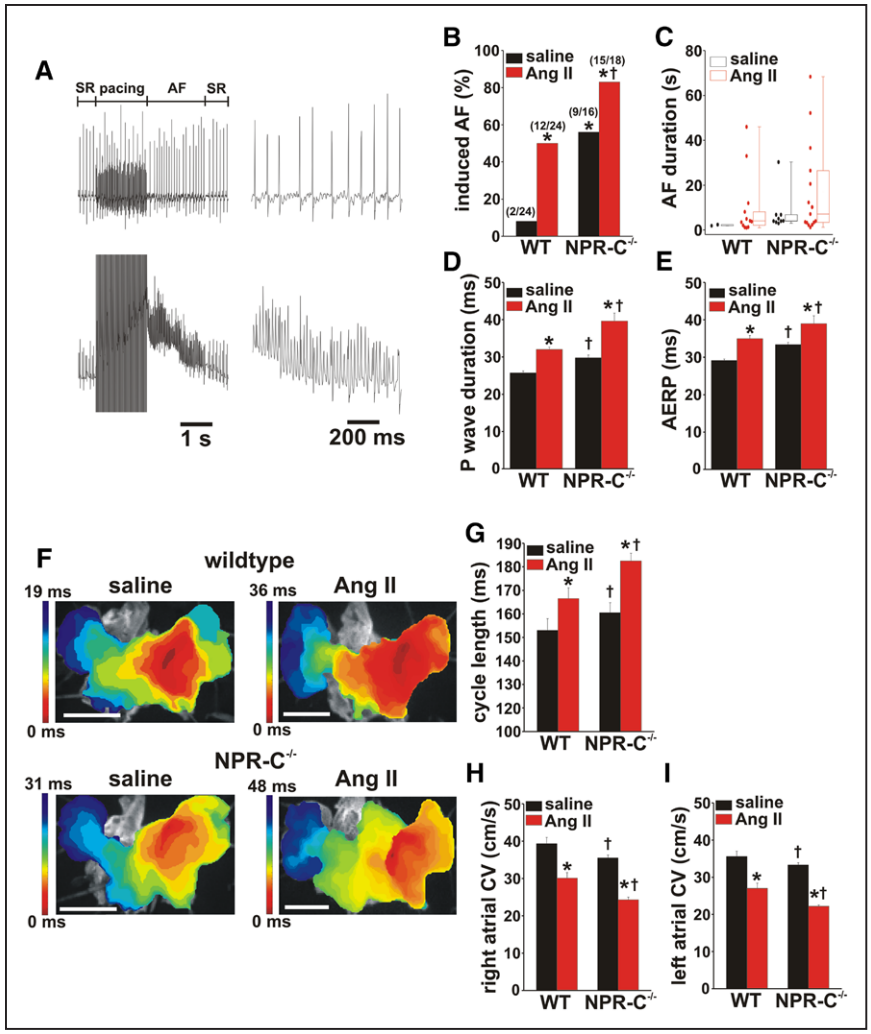

Figure 1. Effects of Ang II (angiotensin II) on inducibility of atrial fibrillation (AF) and atrial electrophysiology in WT (wild type) and NPR-C$^{-/-}$ (natriuretic peptide receptor-C knockout) mice.
A, Representative surface (**top**) and intracardiac atrial (**bottom**) ECGs illustrating the induction of AF after burst pacing in the right atrium (RA). **B**, Inducibility of AF in WT and NPR-C$^{-/-}$ mice treated with saline or Ang II. **P*<0.05 vs saline, †*P*<0.05 vs WT by Fisher exact test. Numbers in parentheses indicate the number of mice induced into AF. **C**, Duration of AF in WT and NPR-C$^{-/-}$ mice treated with saline or Ang II that were induced into AF during burst pacing. Refer to Table I in the Data Supplement for additional AF analysis. **D**, P-wave duration in WT and NPR-C$^{-/-}$ mice treated with saline or Ang II. **P*<0.05 vs saline, †*P*<0.05 vs WT by 2-way ANOVA with Tukey post hoc test. **E**, Atrial node effective refractory period (AERP) in WT and NPR-C$^{-/-}$ mice treated with saline or Ang II. **P*<0.05 vs saline, †*P*<0.05 vs WT by 2-way ANOVA with Tukey post hoc test. **D** and **E**, n=23 mice for WT/saline, 33 mice for WT/Ang II, 14 mice for NPR-C$^{-/-}$/saline, and 15 mice for NPR-C$^{-/-}$/Ang II. **F**, Representative activation maps in isolated atrial preparations from WT and NPR-C$^{-/-}$ mice treated with saline or Ang II. The RA appendage is on the right side of the image; red color indicates initial activation time (scale bars=3 mm). **G**, Effects of Ang II on cycle length in atrial preparations from WT and NPR-C$^{-/-}$ mice. **H** and **I**, RA and left atrial (LA) conduction velocity (CV) as assessed using optical mapping in WT and NPR-C$^{-/-}$ mice treated with saline or Ang II. **G**–**I**, **P*<0.05 vs saline, †*P*<0.05 vs WT by 2-way ANOVA with Tukey post hoc test; n=8 hearts for WT/saline, 8 for WT/Ang II, 5 for NPR-C$^{-/-}$/saline, and 5 for NPR-C$^{-/-}$/Ang II. SR indicates sinus rhythm.

G_{max} was larger (*P*<0.05) in NPR-C$^{-/-}$ mice (Figure VA in the Data Supplement). Similarly, Ang II induced a positive shift (*P*<0.05) in the $V_{1/2(act)}$ that was larger (*P*<0.05) in NPR-C$^{-/-}$ mice compared with wild-type mice (Figure VB in the Data Supplement). These data demonstrating larger effects of Ang II on left atrial I_{Na} in NPR-C$^{-/-}$ mice are consistent with the greater reduction in left atrial AP V_{max} in Ang II–treated NPR-C$^{-/-}$ mice.

We recently demonstrated that Ang II–induced changes in atrial I_{Na} are associated with changes in PKCα expression and activity.[30] Accordingly, we measured the expression of PKCα in the left atrium in wild-type and NPR-C$^{-/-}$ mice after saline or Ang II treatment by Western blotting (Figure 3F). Consistent with a greater reduction in AP V_{max} and I_{Na}, PKCα expression was increased in the left atrium to a greater extent (*P*<0.05) in Ang II–treated NPR-C$^{-/-}$ mice compared with Ang II–treated wild-type mice (Figure 3F). Left atrial PKCα expression was not different (*P*=0.877) between saline-treated wild-type and NPR-C$^{-/-}$ mice.

To investigate the basis for the changes in AP duration, we next measured repolarizing K^+ currents (I_K) in right and left atrial myocytes from saline- and Ang II–treated wild-type and NPR-C$^{-/-}$ mice. Initially, we measured I_K between −100 and +80 mV using voltage clamp protocols with and without a prepulse to −40 mV to inactivate I_{to}.[33,34] Representative recordings for these experiments are presented in Figure VI in the Data Supplement. In right atrial myocytes from wild-type mice, Ang II treatment induced a reduction in repolarizing I_K when measured without a prepulse (Figure 4A), as well as with a prepulse (Figure 4B). Accordingly, the difference currents between these 2 conditions, which is a measurement of I_{to}, demonstrate that I_{to} is reduced in Ang II–treated right atrial myocytes from wild-type mice (Figure 4C). Ang II also reduced (*P*<0.05) I_K in left atrial myocytes in wild-type mice. This is evident in IV curves for I_K measured with and without an inactivating prepulse (Figure 4D and 4E). The difference current (I_{to}) in left atrial myocytes from wild-type mice was reduced (*P*<0.05) after Ang II treatment (Figure 4F). I_K IV curves with and without prepulses, as well as difference currents (as measures of I_{to}), were also measured in right atrial (Figure 4G through 4I) and left atrial (Figure 4J through 4L) myocytes from NPR-C$^{-/-}$ mice treated with saline or Ang II. These data demonstrate that the effects

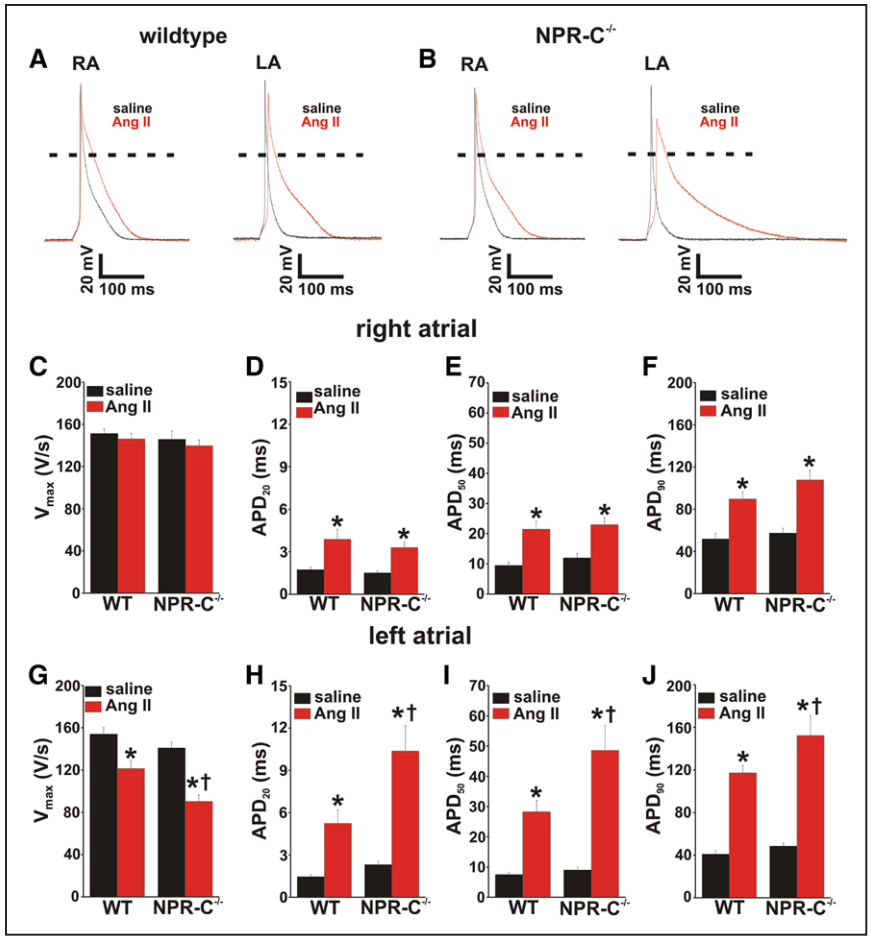

Figure 2. Action potential morphology in right atrial (RA) and left atrial (LA) myocytes from WT (wild type) and NPR-C$^{-/-}$ (natriuretic peptide receptor-C knockout) mice treated with Ang II (angiotensin II). **A** and **B**, Representative stimulated APs in RA and LA myocytes from WT (**A**) and NPR-C$^{-/-}$ (**B**) mice treated with saline or Ang II. **C**, AP V_{max} in RA myocytes from WT and NPR-C$^{-/-}$ mice treated with saline or Ang II. **D**–**F**, AP duration at 20% repolarization (APD_{20}; **D**), 50% repolarization (APD_{50}; **E**), and 90% repolarization (APD_{90}; **F**) in RA myocytes from WT and NPR-C$^{-/-}$ mice treated with saline or Ang II. **C**–**F**, *P<0.05 vs saline by 2-way ANOVA with Tukey post hoc test; n=18 RA myocytes for WT/saline, 15 for WT/Ang II, 23 for NPR-C$^{-/-}$/saline, and 27 for NPR-C$^{-/-}$/Ang II. **G**, AP V_{max} in LA myocytes from WT and NPR-C$^{-/-}$ mice treated with saline or Ang II. **H**–**J**, APD_{20} (**H**), APD_{50} (**I**), and APD_{90} (**J**) in LA myocytes from WT and NPR-C$^{-/-}$ mice treated with saline or Ang II. **G**–**J**, *P<0.05 vs saline, †P<0.05 vs WT by 2-way ANOVA with Tukey post hoc test; n=16 LA myocytes for WT/saline, 18 for WT/Ang II, 16 for NPR-C$^{-/-}$/saline, and 15 for NPR-C$^{-/-}$/Ang II.

of Ang II on I_K in NPR-C$^{-/-}$ mice were similar to wild-type mice. Indeed, direct comparison of I_{to} densities at +50 mV demonstrates that there were no differences in the magnitude of the effect of Ang II between wild-type and NPR-C$^{-/-}$ mice in right (P=0.804) or left (P=0.390) atrial myocytes (Figure VII in the Data Supplement).

We also assessed the ultrarapid delayed rectifier K^+ current (I_{Kur}), which can be measured as the component of I_K that is sensitive to 4-aminopyridine (100 μmol/L).[33,35] I_{Kur} was measured in right and left atrial myocytes from wild-type and NPR-C$^{-/-}$ mice treated with saline or Ang II (Figure VIIIA in the Data Supplement). Summary data demonstrate that I_{Kur} was reduced (P<0.05) after Ang II treatment in right and left atrial myocytes (Figure VIIIB and VIIIC in the Data Supplement). Furthermore, there was no difference in the magnitude of the effect of Ang II on I_{Kur} between wild-type and NPR-C$^{-/-}$ mice in right (P=0.119; Figure VIIIB in the Data Supplement) or left (P=0.897; Figure VIIIC in the Data Supplement) atrial myocytes. We recently demonstrated that Ang II–mediated alterations in I_{to} and I_{Kur} in wild-type mice were not due to changes in expression of the proteins that underlie these channels.[30] This was also investigated here in Ang II–treated NPR-C$^{-/-}$ mice (Figure IX in the Data Supplement). These data demonstrate that Ang II had no effect on protein expression of K_V4.2 (Figure IXA in the Data Supplement), K_V4.3 (Figure IXB in the Data Supplement), KChIP2 (Figure IXC in the Data Supplement), or K_V1.5 (Figure IXD in the Data Supplement) in the right or left atria in NPR-C$^{-/-}$ mice.

Effects of Ang II on Atrial Fibrosis in Wild-Type and NPR-C$^{-/-}$ Mice

We have previously demonstrated that NPR-C$^{-/-}$ mice (untreated) display atrial dysfunction in association with increased atrial fibrosis[20]; however, whether NPR-C affects Ang II–mediated AF in association with changes in atrial fibrosis has not been investigated. Thus, we measured interstitial fibrosis by Picrosirius red staining in the right and left atria of wild-type and NPR-C$^{-/-}$ mice treated with saline or Ang II (Figure 5A and 5B). Summary data demonstrate that Ang II increased (P<0.05) right atrial fibrosis in wild-type and NPR-C$^{-/-}$ mice and that this increase in right atrial fibrosis was larger (P<0.05) in NPR-C$^{-/-}$ mice (Figure 5C). Similar observations were made for left atrial fibrosis (Figure 5D). Notably, the Ang II–induced increase in left atrial fibrosis was larger than in the right atrium, especially in NPR-C$^{-/-}$ mice.

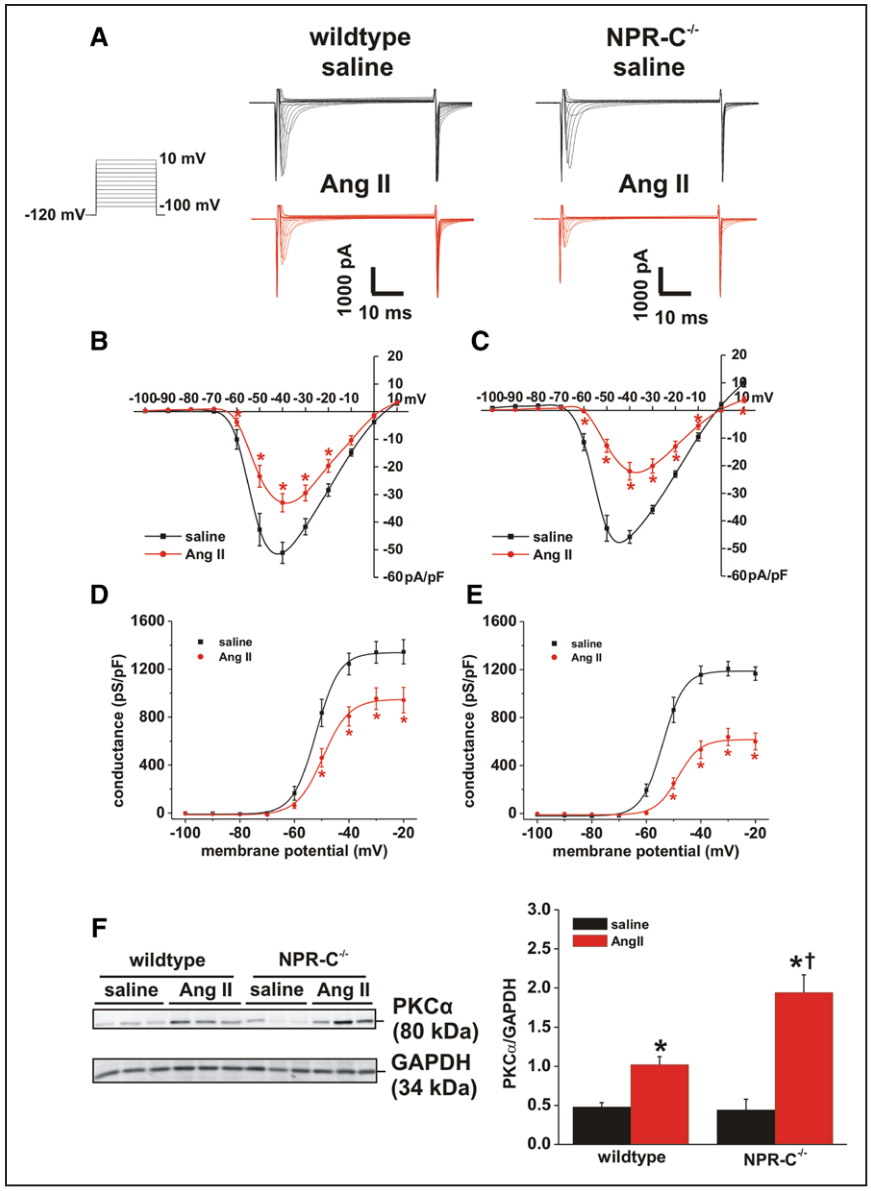

Figure 3. Effects of Ang II (angiotensin II) on left atrial (LA) sodium current in WT (wild type) and NPR-C$^{-/-}$ (natriuretic peptide receptor-C knockout) mice.
A, Representative I_{Na} recordings in LA myocytes from WT and NPR-C$^{-/-}$ mice treated with saline or Ang II. Voltage clamp protocol is shown on the (**left**). **B**, I_{Na} IV curves in LA myocytes from WT mice treated with saline or Ang II. **C**, I_{Na} activation curves for WT mice treated with saline or Ang II. **B** and **C**, *P<0.05 vs saline by 2-way repeated measures ANOVA with Tukey post hoc test; n=9 saline- and 10 Ang II–treated myocytes. **D**, I_{Na} IV curves in LA myocytes from NPR-C$^{-/-}$ mice treated with saline or Ang II. **E**, I_{Na} activation curves for NPR-C$^{-/-}$ mice treated with saline or Ang II. **D** and **E**, *P<0.05 vs saline by 2-way repeated measured ANOVA with Tukey post hoc test; n=9 for saline and 14 for Ang II. Refer to Figure V in the Data Supplement for additional analysis of I_{Na} activation kinetics. **F**, Expression of PKCα (protein kinase Cα) in the LA of WT and NPR-C$^{-/-}$ mice treated with saline or Ang II. *P<0.05 vs saline, †P<0.05 vs WT by 2-way ANOVA with Tukey post hoc test; n=5 for WT/saline, 5 for WT/Ang II, 5 for NPR-C$^{-/-}$/saline, and 7 for NPR-C$^{-/-}$/Ang II.

The basis for Ang II–induced fibrosis in wild-type and NPR-C$^{-/-}$ mice was investigated by measuring the expression of genes involved in fibrosis and fibrotic signaling (Figure 5E). Studies were focused on the gene expression of *Col1a2* and *Col3a1* because these are major interstitial collagens in the myocardium.[14] We also investigated TGFβ and TIMP1, which have both been implicated in Ang II–induced fibrosis in the ventricular myocardium.[36–38] As gene expression changes can begin to manifest early after the initiation of Ang II treatment,[39] we measured gene expression at 3 days and 3 weeks of Ang II treatment in the right and left atria from wild-type and NPR-C$^{-/-}$ mice. In the right atrium after 3 days of Ang II treatment, expression of *Col1a2* and *Col3a1* was higher (P<0.05) in NPR-C$^{-/-}$ mice versus wild-type mice. There was also a tendency for expression of these collagen genes to be higher after Ang II treatment in NPR-C$^{-/-}$ but not wild-type right atria (Figure 5E). At the 3-day time point, *TGFβ* expression was elevated (P<0.05) in the right atria in NPR-C$^{-/-}$ mice, and there was also a clear trend (P=0.054) toward increased right atrial *TGFβ* after Ang II treatment in NPR-C$^{-/-}$ mice (Figure 5E). Strikingly, Ang II induced a substantial increase (P<0.05) in expression of *Timp1* in the right atrium of NPR-C$^{-/-}$ mice but not wild-type mice (P=0.867) at 3 days (Figure 5E) of Ang II treatment. Summary data for gene expression changes in the right atrium after 3 weeks of Ang II treatment indicate that the Ang II–induced changes observed at 3 days were no longer present (Figure 5E). Specifically, 3 weeks after initiation of Ang II, there were no differences in right atrial expression of *TGFβ* (P=0.322) or *Timp1* (P=0.277) in wild-type or NPR-C$^{-/-}$ mice.

In the left atrium, 3 days of Ang II treatment increased (P<0.05) *Col1a2* expression in wild-type and NPR-C$^{-/-}$ mice, with greater increases (P<0.05) in mice lacking NPR-C (Figure 5E). *Col3a1* was also increased (P<0.05)

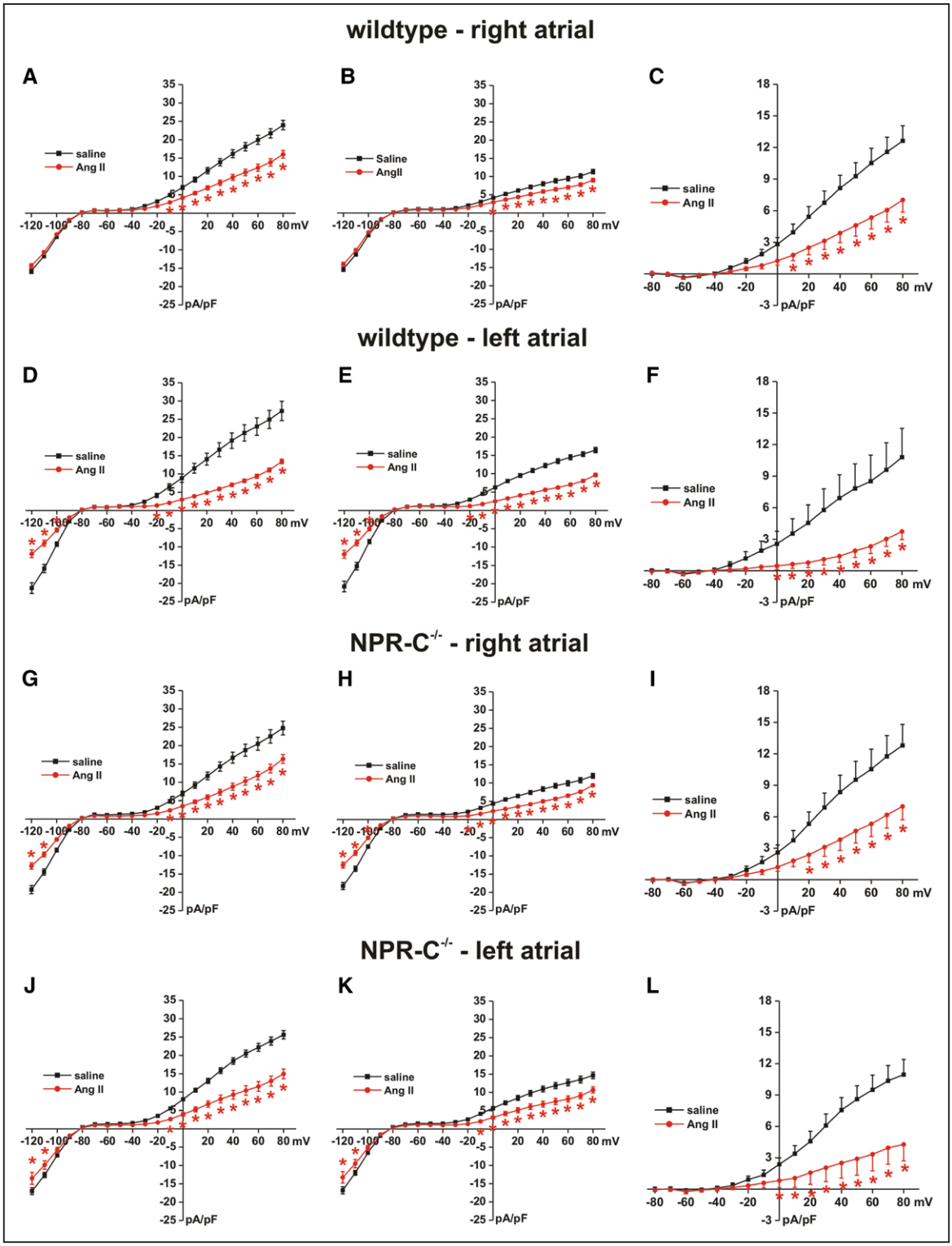

Figure 4. Effects of Ang II (angiotensin II) on atrial potassium currents in WT (wild type) and NPR-C$^{-/-}$ (natriuretic peptide receptor-C knockout) mice.

I_K was recorded with and without a prepulse to –40 mV to inactivate I_{to}. Representative I_K recordings from right atrial (RA) and left atrial (LA) myocytes isolated from WT and NPR-C$^{-/-}$ mice treated with saline or Ang II are located in Figure VI in the Data Supplement. **A**–**C**, I_K IV curves for RA myocytes from WT mice are shown for the peak of the I_K recordings without the prepulse (**A**), the peak of the I_K recordings with the prepulse (**B**), and the difference current between (**A**) and (**B**), which is a measure of I_{to} (**C**). **A**–**C**, **P*<0.05 vs saline by 2-way repeated measures ANOVA with Tukey post hoc test; n=29 RA myocytes for saline and 16 for Ang II. **D**–**F**, I_K IV curves for left atrial myocytes from WT mice are shown for the peak of the I_K recordings without the prepulse (**D**), the peak of the I_K recordings with the prepulse (**E**), and the difference current between (**D**) and (**E**), which is a measure of I_{to} (**F**). **D**–**F**, **P*<0.05 vs saline by 2-way repeated measures ANOVA with Tukey post hoc test; n=12 left atrial myocytes for saline and 20 for Ang II. **G**–**I**, I_K IV curves for RA myocytes from NPR-C$^{-/-}$ mice are shown for the peak of the I_K recordings (*Continued*)

after 3 days of Ang II in wild-type and NPR-C$^{-/-}$ left atria. *TGFβ* expression was increased (P<0.05) after 3 days of Ang II in the left atrium of wild-type mice and increased to a greater extent (P<0.05) in the left atrium of NPR-C$^{-/-}$ mice. Three days of Ang II treatment induced a large increase (P<0.05) in *Timp1* expression in the left atrium of wild-type mice and, consistent with the right atrium, a much larger increase (P<0.05) in NPR-C$^{-/-}$ mice (Figure 5E). In contrast to the right atrium, the increases in expression of *Col1a2* and *Col3a1* in the left atrium were maintained after 3 weeks of Ang II treatment (Figure 5E). After 3 weeks of Ang II treatment, *TGFβ* expression in the left atrium was increased (P<0.05) only in Ang II–treated NPR-C$^{-/-}$ mice. On the contrary, *Timp1* expression remained elevated (P<0.05) in wild-type and NPR-C$^{-/-}$ left atria after 3 weeks of Ang II. Furthermore, there was a clear trend (P=0.058) for *Timp1* expression in the left atrium to remain higher in Ang II–treated NPR-C$^{-/-}$ mice compared with Ang II–treated wild-type mice at 3 weeks (Figure 5E).

In addition to TIMP1, TIMP2, TIMP3, and TIMP4 are also present in the heart where they can play important roles in regulation of the extracellular matrix and fibrosis.[14] Accordingly, we also measured the expression of *Timp2*, *Timp3*, and *Timp4* in the right and left atria of wild-type and NPR-C$^{-/-}$ mice at the same time points as above (Figure X in the Data Supplement). These data demonstrate some changes in TIMP2, TIMP3, and TIMP4 among treatment groups, but these did not correlate with the increases in atrial fibrosis we observed in Ang II–treated NPR-C$^{-/-}$ mice compared with Ang II–treated wild-type mice. Thus, our data suggest that TIMP1 may be of particular importance in mediating Ang II–induced atrial fibrosis and that TIMP1 expression is affected by loss of NPR-C (see Discussion).

NPR-C Activation Protects Against AF and Atrial Electrical Dysfunction

The data presented above demonstrate that loss of NPR-C results in increased susceptibility to Ang II–mediated AF and more severe changes in Ang II–induced electrical dysfunction in the atria, suggesting an important protective role for NPR-C. Accordingly, the next series of experiments was designed to test the hypothesis that cotreating wild-type mice with Ang II and an NPR-C activator would prevent the effects of Ang II in the atria. These studies were performed using the selective NPR-C agonist cANF at doses of 0.07 and 0.14 mg/kg per day. These doses were selected based on previous studies in which NPs were administered clinically and in animal studies.[24,32]

First, we measured the gene and protein expression of NPR-A, NPR-B, and NPR-C in the right and left atria of wild-type mice treated with saline or Ang II. These studies show that the mRNA expression of *Npr1* (encodes NPR-A), *Npr2* (encodes NPR-B), and *Npr3* (encodes NPR-C) was not affected by Ang II treatment in the right or left atria compared with saline controls (Figure XI in the Data Supplement); however, Npr3 expression was lower (P<0.05) in the left atrium compared with the right atrium in Ang II–treated mice (Figure XI in the Data Supplement). Western blotting studies show that Ang II had no effects on the expression of NPR-A, NPR-B, or NPR-C in the right atrium (Figure XIIA and XIIB in the Data Supplement). On the contrary, protein expression of NPR-A and NPR-B was reduced (P<0.05) in the left atrium after Ang II treatment. NPR-C protein expression in the left atrium also showed a trend toward reduction (P=0.055) after Ang II treatment (Figure XIIA and XIIC in the Data Supplement).

Next, the effects of cANF cotreatment with Ang II on systolic blood pressure were measured. These data demonstrate that systolic blood pressure was increased (P<0.05) in mice treated with Ang II alone and in mice treated with Ang II with cANF at both doses (Figure XIII in the Data Supplement). There were no differences (P=0.267) in the magnitude of the increase in systolic blood pressure after treatment with Ang II alone or Ang II with cANF at either dose (Figure XIII in the Data Supplement) indicating that cANF did not prevent Ang II–mediated hypertension.

The effects of cANF cotreatment on inducibility of AF and atrial electrophysiology were investigated next. These data demonstrate that cotreating wild-type mice with Ang II and the lower dose of cANF (0.07 mg/kg per day) did not affect susceptibility to AF, which was increased (P<0.05) in both groups compared with saline-treated mice (Figure 6A). AF durations in mice treated with Ang II alone or Ang II with cANF (0.07 mg/kg per day) were also similar (Figure 6B; Table V in the Data Supplement). Conversely, cotreating mice with Ang II and a higher dose of cANF (0.14 mg/kg per day) potently reduced (P<0.05) the susceptibility to AF compared with mice treated with Ang II alone, as well as Ang II with the lower dose of cANF (Figure 6A). Furthermore, when AF was induced in mice cotreated with Ang II and the higher dose of cANF (0.14 mg/kg per day), it was brief, lasting <5 s in all cases (Figure 6B; Table V in the Data Supplement).

Analysis of ECG parameters (Table VI in the Data Supplement) demonstrates that P-wave duration was increased (P<0.05) in mice treated with Ang II and the lower dose of cANF (0.07 mg/kg per day) compared with saline controls and not different (P=0.977) from

Figure 4 Continued. without the prepulse (**G**), the peak of the I_K recordings with the prepulse (**H**), and the difference current between (**G**) and (**H**), which is a measure of I_{to} (**I**). **G**–**I**, *P<0.05 vs saline by 2-way repeated measures ANOVA with Tukey post hoc test; n=16 RA myocytes for saline and 23 for Ang II. **J**–**L**, I_K IV curves for left atrial myocytes from NPR-C$^{-/-}$ mice are shown for the peak of the I_K recordings without the prepulse (**J**), the peak of the I_K recordings with the prepulse (**K**), and the difference current between (**J**) and (**K**), which is a measure of I_{to} (**L**). **J**–**L**, *P<0.05 vs saline by 2-way repeated measures ANOVA with Tukey post hoc test; n=17 left atrial myocytes for saline and 13 for Ang II.

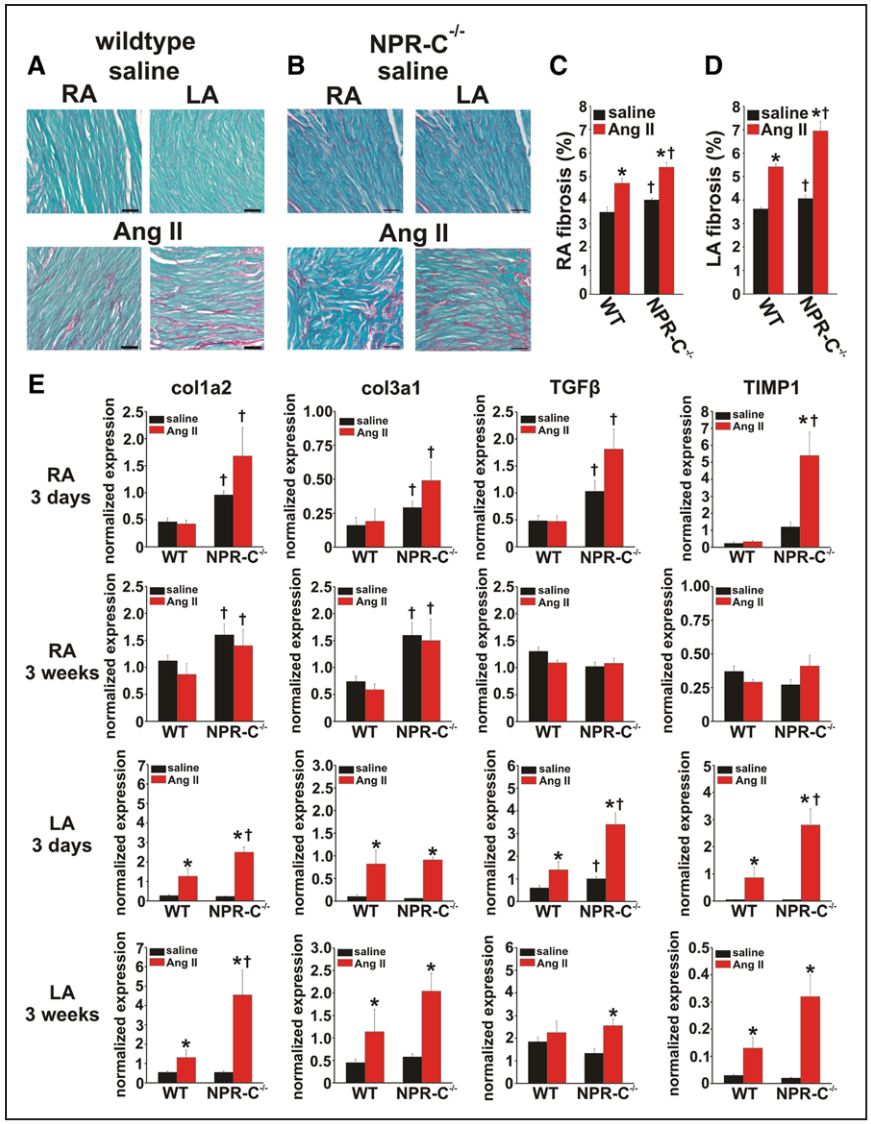

Figure 5. Effects of Ang II (angiotensin II) on interstitial fibrosis in the atria in WT (wild type) and NPR-C$^{-/-}$ (natriuretic peptide receptor-C knockout) mice.
A and **B**, Representative images demonstrating patterns of interstitial fibrosis (collagen fibers in red) in the right atria (RA) and left atria (LA) for WT (**A**) and NPR-C$^{-/-}$ (**B**) mice treated with saline or Ang II. **C** and **D**, Summary of interstitial fibrosis in the RA (**C**) and LA (**D**). *P<0.05 vs saline, †P<0.05 vs WT by 2-way ANOVA with Tukey post hoc test; n=5 for WT/saline, 5 for WT/Ang II, 5 for NPR-C$^{-/-}$/saline, and 8 for NPR-C$^{-/-}$/Ang II. **E**, mRNA expression of col1a2 (collagen type I), col3a1 (collagen type III), TGFβ (transforming growth factor β), and TIMP1 (tissue inhibitor of metalloproteinase 1) in the RA and LA after 3 d and 3 wk of Ang II or saline treatment. *P<0.05 vs saline within genotype, †P<0.05 vs WT within treatment group by 2-way ANOVA with Tukey post hoc test; n=6 for WT/saline, 8 for WT/Ang II, 6 for NPR-C$^{-/-}$/saline, and 8 for NPR-C$^{-/-}$/Ang II.

mice treated with Ang II alone (Figure 6C). Cotreatment with the higher dose of cANF resulted in intermediate P-wave durations that were reduced (P<0.05) compared with Ang II alone but still greater (P<0.05) than saline-treated mice (Figure 6C). AERP was not different in mice treated with Ang II and cANF at doses of 0.07 (P=0.878) or 0.14 mg/kg per day (P=0.974) compared with Ang II alone (Figure 6D).

The effects of cANF cotreatment on atrial conduction were also assessed using high-resolution optical mapping in isolated atrial preparations in sinus rhythm (Figure 6E). Summary data demonstrate that the higher dose of cANF (0.14 mg/kg per day) prevented (P<0.05) the Ang II–induced prolongation in cycle length (Figure 6F). Furthermore, these data demonstrate the lower dose of cANF (0.07 mg/kg per day) resulted in intermediate CVs in the right atrium, which were increased (P<0.05) compared with Ang II but still lower (P<0.05) than saline (Figure 6G). The higher dose of cANF (0.14 mg/kg per day) increased right atrial CV compared with Ang II alone (P<0.05) and these CVs trended toward being higher than the lower dose of cANF (P=0.061), and were similar to saline-treated mice (Figure 6G). Left atrial CV was increased (P<0.05) after cotreatment with the higher dose of cANF (0.14 mg/kg per day) but not the lower dose of cANF (0.07 mg/kg per day; Figure 6H). Left atrial CV also remained reduced (P<0.05) after cotreatment with both doses of cANF compared with saline-treated mice (Figure 6H). Analysis of AP duration from optical APs (Figure XIVA and XIVB in the Data Supplement) demonstrates that the higher dose of cANF (0.14 mg/kg per day) prevented (P<0.05) the Ang II–induced prolongation of APD_{50} (Figure XIVC in the Data Supplement) and APD_{70} (Figure XIVD in the Data Supplement) in the right atrium. The lower dose of cANF (0.07 mg/kg per day) did not affect right atrial APD_{50} (P=0.234) or APD_{70} (P=0.121) compared with Ang II alone (Figure XIVC and XIVD in the Data Supplement). In the left atrium, cotreatment with either dose of cANF did not affect APD_{50} (P=0.998 for 0.07 mg/kg per day cANF; P=0.349 for 0.14 mg/kg

per day cANF; Figure XIVE in the Data Supplement) or APD_{70} (P=0.883 for 0.07 mg/kg per day cANF; P=0.336 for 0.14 mg/kg per day cANF; Figure XIVF in the Data Supplement) compared with Ang II alone.

Effects of cANF on Atrial AP Morphology and Atrial Fibrosis

Because the effects of cANF on AF and atrial electrophysiology were evident primarily at the higher dose of 0.14 mg/kg per day, we measured the effects of this dose of cANF on AP morphology in isolated right and left atrial myocytes (Figure 7A) from wild-type mice. Consistent with the data presented earlier, AP V_{max} was not altered (P=0.293) in right atrial myocytes from mice treated with Ang II alone or Ang II with cANF. In left atrial myocytes, AP V_{max} remained reduced (P<0.05) in mice treated with Ang II and cANF compared with saline controls and was not different (P=0.876) from Ang II alone (Figure 7B). In right atrial myocytes from mice cotreated with Ang II and cANF APD_{20} (Figure 7C), APD_{50} (Figure 7D) and APD_{90} (Figure 7E) were each reduced (P<0.05) compared with mice treated with Ang II alone. After cotreatment with cANF APD_{20} (P=0.648), APD_{50} (P=0.486) and APD_{90} (P=0.707) in right atrial myocytes were not different from saline controls, indicating a significant improvement in right atrial myocyte AP morphology after NPR-C activation (Table VII in the Data Supplement). In contrast, APD_{20} (P=0.234), APD_{50} (P=0.205), and APD_{90} (P=0.982) values in the left atrium were not affected by cANF cotreatment compared with Ang II alone (Figure 7C through 7E; Table VIII in the Data Supplement).

Consistent with the improvements in right atrial AP morphology, cotreating mice with cANF (0.14 mg/kg per day) also prevented the Ang II–induced reduction in I_K in right atrial myocytes (Figure 7F). Summary IV curves for I_K recordings with and without an inactivating prepulse demonstrate that I_K was larger (P<0.05) in right atrial myocytes from mice cotreated with Ang II and cANF (0.14 mg/kg per day) compared with Ang II alone (Figure 7G and 7H). Similarly, the Ang II–induced reduction in right atrial I_{to} was completely prevented by cotreatment with cANF (0.14 mg/kg per day; Figure 7I). Conversely, cotreatment with Ang II and cANF (0.14 mg/kg per day) had no effects on I_K, including I_{to}, in left atrial myocytes (Figure XV in the Data Supplement), and cANF cotreatment did not prevent the Ang II–induced increase in cell capacitance in left atrial myocytes (Figure XVI in the Data Supplement).

Finally, we investigated the effects of cANF cotreatment (at doses of 0.07 and 0.14 mg/kg per day) on right and left atrial fibrosis (Figure 8A). Summary data demonstrate that cotreatment with cANF at doses of 0.07 (P=0.519) and 0.14 mg/kg per day (P=0.269) reduced (P<0.05) right atrial fibrosis compared with Ang II alone to levels that were no different from saline-treated mice (Figure 8B). In left atrial myocytes, cotreatment with the lower dose of cANF (0.07 mg/kg per day) resulted in intermediate levels of fibrosis (Figure 8C) that were not different from Ang II alone (P=0.238) or saline (P=0.539). However, the higher dose of cANF (0.14 mg/kg per day) strongly prevented (P<0.05) the Ang II–induced increase in left atrial fibrosis, which was not different (P=1.000) from saline controls (Figure 8C).

DISCUSSION

Ang II and hypertension are well known to be associated with AF, and Ang II treatment in mice is a well-established model of AF and atrial remodeling.[2,5,30,40,41] Consistent with this, we recently demonstrated that Ang II treatment in mice increases susceptibility to AF in association with distinct patterns of electrical remodeling in the right and left atria, as well as increases in fibrosis in both atria.[30] Strikingly, in the present study, we demonstrate that loss of NPR-C greatly exacerbates Ang II–mediated alterations in atrial electrophysiology, conduction, and arrhythmogenesis, whereas cotreatment with the NPR-C agonist cANF was protective. Notably, the alterations in atrial function in NPR-C$^{-/-}$ mice and the effects of NPR-C activation with cANF occurred without differences in the degree of hypertension elicited by Ang II. This indicates that the effects of modulating NPR-C activity occur directly within the atria, independent of any effects on blood pressure. These results identify a previously unknown role for NPR-C in the progression of Ang II–induced AF, suggesting that NPR-C could be a novel target within the atria to protect against the progression of Ang II–mediated atrial dysfunction.

We recently demonstrated that Ang II also induces sinoatrial node disease and that this too is worsened in Ang II–treated NPR-C$^{-/-}$ mice.[32] In this same study, we found that 3 weeks of Ang II treatment in wild-type mice caused cardiac hypertrophy with preserved systolic function whereas Ang II treatment in NPR-C$^{-/-}$ mice resulted in ventricular dilation and overt systolic heart failure.[32] AF and sinoatrial node disease frequently coexist,[42,43] and AF is also common in heart failure[2]; therefore, our observations that AF inducibility and severity are worsened in Ang II–treated NPR-C$^{-/-}$ mice are consistent with more severe declines in sinoatrial node function and more rapid development of heart failure after Ang II treatment in the absence of NPR-C.

Our studies demonstrate that NPR-C modulates Ang II electrical and structural remodeling in the atria. In terms of electrical remodeling, we found that Ang II caused prolongations in AP duration in the right and left atria and a reduction in V_{max} in the left atrium only. AP prolongation in the right atrium was similar between wild-

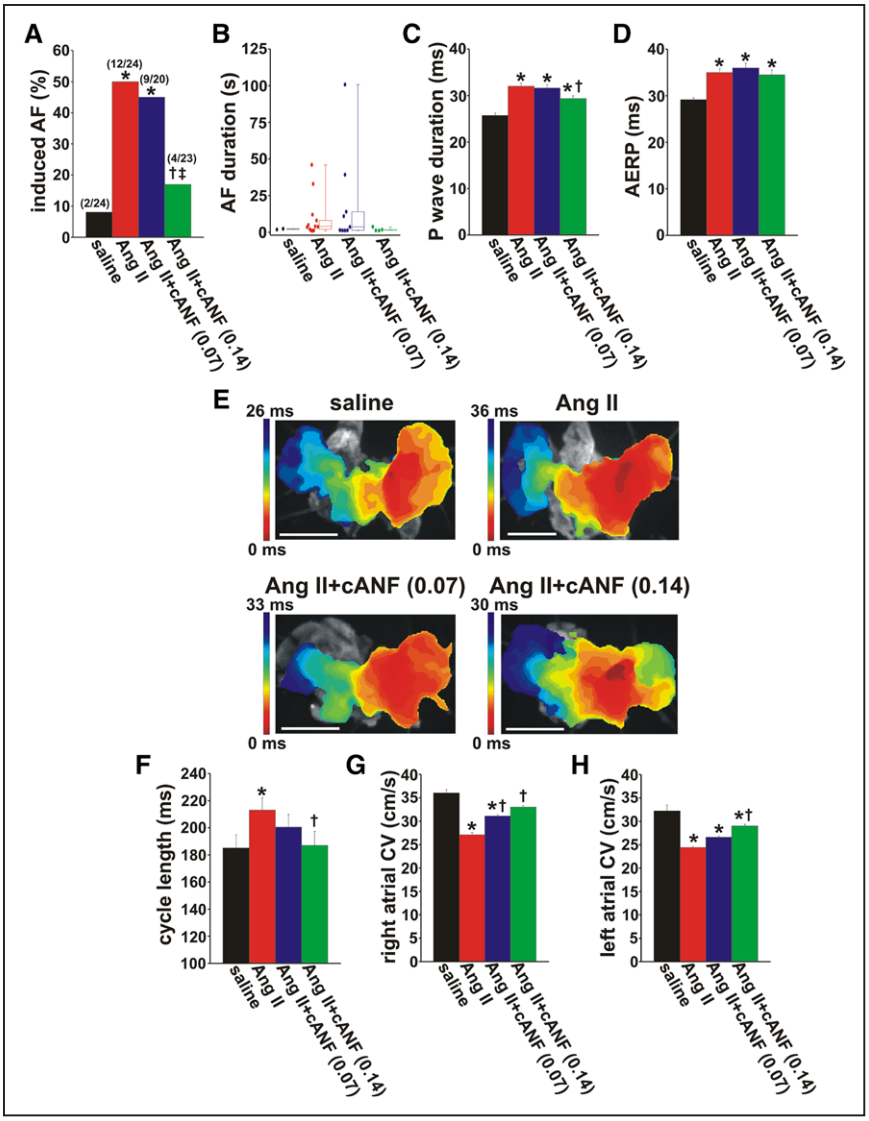

Figure 6. Effects of cotreatment with Ang II (angiotensin II) and the NPR-C (natriuretic peptide receptor-C) agonist cANF on inducibility of atrial fibrillation (AF) and atrial electrophysiology.

A, Inducibility of AF in WT (wild type) mice treated with saline, Ang II, or Ang II with cANF (0.07 or 0.14 mg/kg per d). **P*<0.05 vs saline, †*P*<0.05 vs Ang II, ‡*P*<0.05 vs Ang II+cANF (0.07) by Fisher exact test. Numbers in parentheses indicate the number of mice induced into AF. **B**, Duration of AF in WT mice treated with saline, Ang II, or Ang II with cANF (0.07 or 0.14 mg/kg per d) that were induced into AF. Refer to Table V in the Data Supplement for additional information on AF durations. **C** and **D**, P-wave duration (**C**) and atrial effective refractory period (AERP; **D**) in WT mice treated with saline, Ang II, or Ang II with cANF (0.07 or 0.14 mg/kg per d). **C** and **D**, **P*<0.05 vs saline, †*P*<0.05 vs Ang II by 1-way ANOVA with Tukey post hoc test; n=23 mice for saline, 33 for Ang II, 20 for Ang II+cANF (0.07), and 22 for Ang II+cANF (0.14). **E**, Representative activation maps in isolated atrial preparations from WT mice treated with saline, Ang II, or Ang II with cANF (0.07 or 0.14 mg/kg per d; scale bars=3 mm). **F**, Effects of cANF cotreatment on atrial cycle length. **G** and **H**, Right and left atrial conduction velocity (CV) in WT mice treated with saline, Ang II, or Ang II with cANF (0.07 or 0.14 mg/kg per d). **F**–**H**, **P*<0.05 vs saline, †*P*<0.05 vs Ang II by 1-way ANOVA with Tukey post hoc test; n=9 for saline, 9 for Ang II, 7 for Ang II+cANF (0.07), and 8 for Ang II+cANF (0.14).

type and NPR-C$^{-/-}$ mice treated with Ang II, as shown in optical mapping and patch-clamp studies. On the contrary, Ang II–treated NPR-C$^{-/-}$ mice exhibited larger reductions in V_{max} and greater AP prolongation in the left atrium, indicating that loss of NPR-C exacerbated electrical remodeling, especially in the left atrium. More substantial changes in left atrial AP morphology in Ang II–treated NPR-C$^{-/-}$ mice were confirmed in intact atria by optical mapping, as well as in isolated atrial myocytes by patch clamp. These findings are in agreement with greater prolongations in P-wave duration and AERP in Ang II–treated NPR-C$^{-/-}$ mice in vivo. The greater reduction in left atrial V_{max} was associated with a larger reduction in left atrial I_{Na} and greater increases in PKCα expression in Ang II–treated NPR-C$^{-/-}$ mice. These observations are consistent with our recent study showing that the Ang II–induced reduction in atrial I_{Na} in wild-type mice can be reversed by inhibiting PKC and that I_{Na} is only reduced in left atrial myocytes after Ang II treatment in wild-type mice.[30] These previous findings, in conjunction with our present study, indicate that changes in PKCα expression and PKC activity account for the differential effects of Ang II on I_{Na} in left and right atria.

Interestingly, despite a greater prolongation of AP duration, we observed no differences in the degree of reduction in repolarizing I_K, including I_{to} and I_{Kur}, in Ang II–treated left atrial myocytes from wild-type and NPR-C$^{-/-}$ mice. We have also previously found that $I_{Ca,L}$ is not altered in right or left atrial myocytes in Ang II–treated mice.[30] Thus, the increase in AP duration in the left atrium in Ang II–treated NPR-C$^{-/-}$ mice must be explained by other mechanisms. One possibility is that the reductions in I_{Na} and AP V_{max}, which result in less depolarization during the AP, could lead to less voltage-dependent activation of repolarizing K^+ currents, including I_{to} and I_{Kur}. We previously demonstrated that reductions in I_{to} and I_{Kur} in the atria of wild-type mice after Ang II treatment were not associated with changes in the expression of the proteins that underlie these channels.[30] Rather, they occurred because of changes

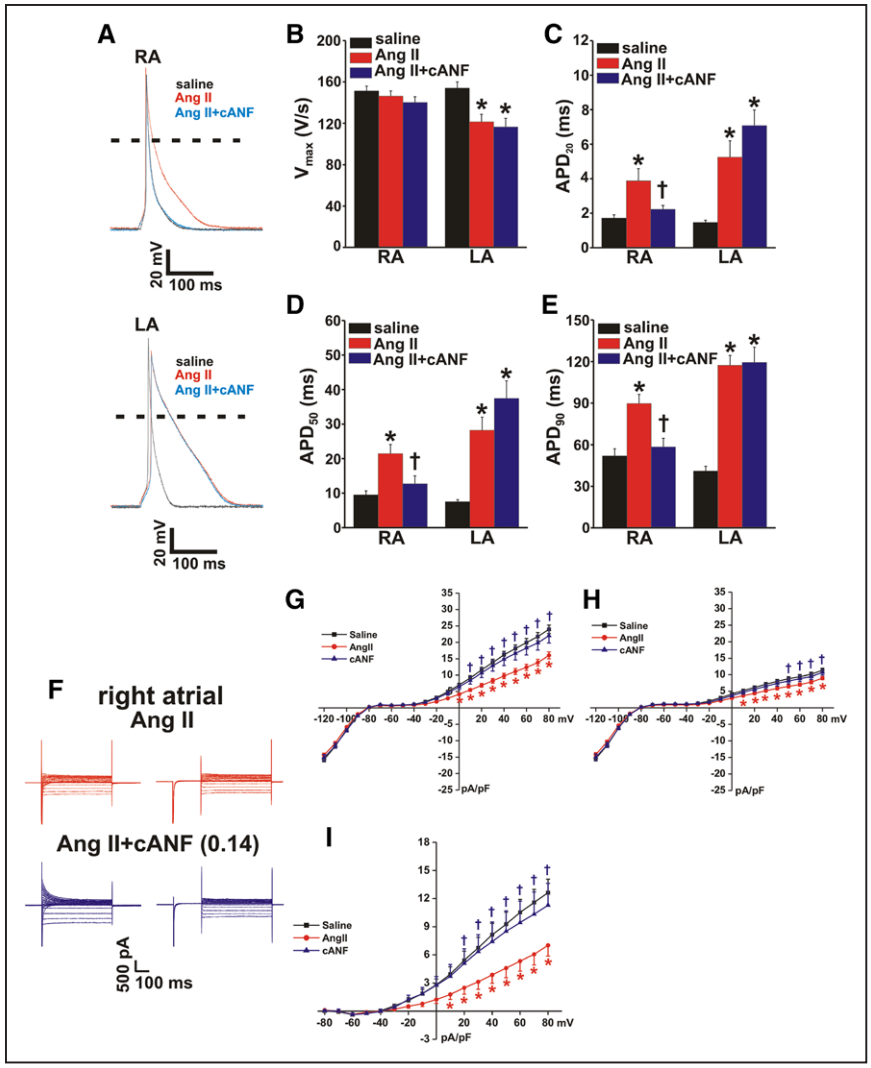

Figure 7. Effects of cotreatment with Ang II (angiotensin II) and cANF on atrial myocyte action potential morphology and K^+ currents.

A, Representative stimulated APs in right atrial (RA) and left atrial (LA) myocytes from WT (wild type) mice treated with saline, Ang II, or Ang II+cANF (0.14 mg/kg per d). **B**, AP V_{max} in RA and LA myocytes from WT mice treated with saline, Ang II, or Ang II+cANF (0.14 mg/kg per d). **C**–**E**, AP duration at 20% repolarization (APD_{20};**C**), APD_{50} (**D**), and APD_{90} (**E**) in RA and LA myocytes from WT mice treated with saline, Ang II, or Ang II+cANF (0.14 mg/kg per d). **B**–**E**, **P*<0.05 vs saline, †*P*<0.05 vs Ang II by 1-way ANOVA with Tukey post hoc test within atrial region; n=18 for saline, 15 for Ang II, and 17 for Ang II+cANF (0.14 mg/kg per d) for RA myocytes; n=16 for saline, 18 for Ang II, and 18 for Ang II+cANF (0.14) for LA myocytes. **F**, Representative I_K recordings with and without an inactivating prepulse in RA myocytes from mice treated with Ang II alone or Ang II+cANF (0.14 mg/kg per d). **G**, Summary I_K IV curves measured at the peak of the I_K recordings without the prepulse in RA myocytes from mice treated with saline, Ang II, or Ang II+cANF (0.14 mg/kg per d). **H**, Summary I_K IV curves measured at the peak of the I_K recordings with the prepulse in RA myocytes from mice treated with saline, Ang II, or Ang II+cANF (0.14 mg/kg per d). **I**, Summary I_{to} IV curves (the difference current between **G** and **H**) in RA myocytes from mice treated with saline, Ang II, or Ang II+cANF (0.14 mg/kg per d). **G**–**I**, **P*<0.05 vs saline, †*P*<0.05 vs Ang II by 1-way repeated measures ANOVA with Tukey post hoc test; n=29 RA myocytes for saline, 28 for Ang II, and 14 for Ang II+cANF (0.14 mg/kg per d).

in biophysical properties of the currents. In the present study, we extend these findings to Ang II–treated NPR-$C^{-/-}$ mice and confirm that Ang II treatment did not alter the protein levels of $K_V4.2$, $K_V4.3$, KChIP2, or $K_V1.5$ in the right or left atria in NPR-$C^{-/-}$ mice.

We also found that loss of NPR-C greatly exacerbates right and left atrial fibrosis, with the highest levels of fibrosis occurring in the left atrium. We investigated the mechanisms for these findings and identified changes in expression of genes for Col1a2 and Col3a1, TGFβ, and TIMP1. Specifically, Ang II–treated NPR-$C^{-/-}$ mice exhibited larger increases in expression of TGFβ than wild-type mice in the right and left atria that were evident after 3 days of Ang II treatment, but which had largely dissipated by 3 weeks of Ang II treatment. TGFβ is a well-known profibrotic signaling molecule[37,44] that has been previously implicated in atrial fibrosis and AF.[45] We also found that NPR-$C^{-/-}$ mice treated with Ang II showed substantial increases in TIMP1 expression in the right and left atria at 3 days. Furthermore, TIMP1 expression remained elevated in the left atrium even after 3 weeks of Ang II treatment. The continued presence of gene expression changes in the left atrium, but not the right atrium, after 3 weeks of Ang II treatment is consistent with greater fibrosis in the left atrium. Because TIMP1 showed the greatest increase in terms of fold change in expression and because its expression remained elevated in the left atrium when other gene expression changes had dissipated, TIMP1 may be playing a key role in Ang II–mediated fibrosis in NPR-$C^{-/-}$ mice. Consistent with this, TIMP1 has recently been shown to play a critical role in Ang II–mediated ventricular fibrosis, independent of effects on MMPs.[38]

The changes in *TGFβ* and *Timp1* expression we observed were associated with changes in expression of *Col1a2* and *Col3a1* that were especially evident in the left atrium. In the present study, we also observed changes in expression of other TIMPs (eg, TIMP3) in the right and left atria in wild-type mice. Although these changes do not seem to underlie the enhanced fibrotic response in NPR-$C^{-/-}$ mice, they could contribute to increases in right and left atrial fibrosis that occur independently of changes in collagen gene expression. For example, a reduction in TIMP3, which we observed

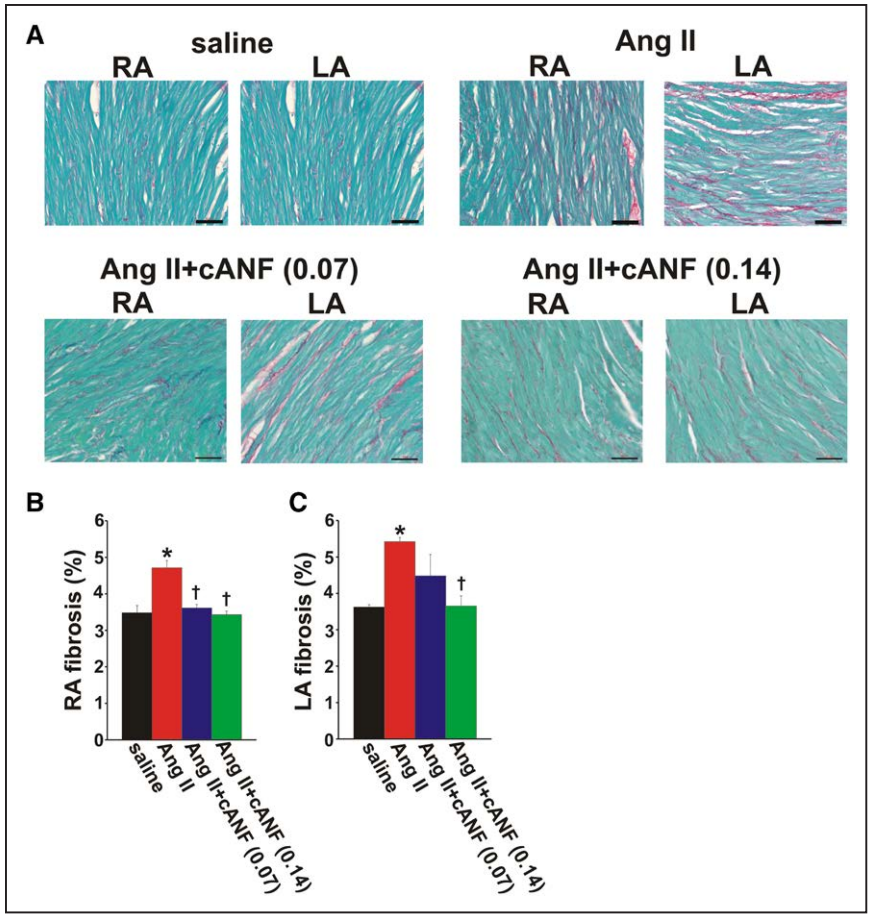

Figure 8. Effects of the NPR-C (natriuretic peptide receptor-C) agonist cANF on Ang II (angiotensin II)–mediated atrial fibrosis. **A**, Representative images demonstrating patterns of interstitial fibrosis in right atria (RA) and left atria (LA) from WT (wild type) mice treated with saline, Ang II, Ang II+cANF (0.07 mg/kg per d), and Ang II+cANF (0.14 mg/kg per d). **B** and **C**, Summary of interstitial fibrosis in the RA (**B**) and LA (**C**) in WT mice treated with saline, Ang II, Ang II+cANF (0.07 mg/kg per d), and Ang II+cANF (0.14 mg/kg per d). **P*<0.05 vs saline, †*P*<0.05 vs Ang II by 1-way ANOVA with Tukey post hoc test; n=5 for saline, 5 for Ang II, 7 for Ang II+cANF (0.07 mg/kg per d), and 5 for Ang II+cANF (0.14 mg/kg per d).

in the right and left atria after 3 weeks of Ang II treatment, is consistent with increases in ventricular fibrosis in TIMP3 knockout mice.[46]

Our study also demonstrates that activating NPR-C with cANF potently reduced the susceptibility to AF, greatly decreased the duration of AF when it occurred, and prevented some of the impairments in atrial conduction induced by Ang II in wild-type mice. Interestingly, our optical mapping studies and our patch-clamp studies illustrate that cANF dose dependently prevented the Ang II–induced alterations in right atrial AP morphology, as well as the reduction in right atrial I_K but not the changes in left atrial AP morphology. As such, left atrial V_{max} (and presumably I_{Na}) remained reduced after cANF cotreatment, and cANF had no effect on left atrial AP duration or I_K. On the contrary, cANF effectively prevented Ang II–mediated fibrosis in the right and left atria in wild-type mice. Collectively, these findings suggest that the reduction in fibrosis throughout the atria, as well as the improvements in right atrial AP morphology induced by cANF cotreatment, is sufficient to decrease the likelihood of AF initiation and maintenance, despite the fact that impairments in left atrial AP morphology persist. Although left atrial CV was clearly improved by cANF cotreatment, it was not fully normalized, presumably because left atrial I_{Na} was still reduced. These findings suggest that targeting and reducing fibrosis with cANF is an effective approach to improving right and left atrial CV and that this reduces susceptibly to AF, despite the reduction in left atrial I_{Na}. Fibrosis is well recognized as a determinant of impaired electrical conduction and atrial arrhythmogenesis[3,12,13]; therefore, reducing fibrosis and preventing a decline in CV would be expected to decrease the likelihood of reentry by increasing the wavelength.[2,11] Although a prolongation of the AP duration could result in early afterdepolarizations,[2] this may not lead to maintained AF if the underlying substrate is sufficiently improved by reducing fibrosis. Furthermore, although AF is thought to be more commonly triggered in the left atrium, the right atrium can also be a source of triggered activity.[47–49] Thus, cANF could also decrease AF susceptibility through its ability to prevent prolongations in right atrial AP duration.

The reason why cANF cotreatment was able to prevent Ang II–mediated electrical remodeling in right but not left atrial myocytes is currently unknown. Our data do suggest that disease progression was greater in the left atrium, as indicated by increases in cell capacitance and more extensive changes in AP morphology. This may contribute to left atrial myocytes being more refractory to the effects of cANF. Consistent with this hypothesis, we did observe a modest reduction in NPR-C protein expression in the left atrium (but not the right atrium) after Ang II treatment. Furthermore, *Npr3* gene expres-

sion was lower in the left atrium compared with the right atrium after Ang II treatment. These alterations may contribute to differential effects of NPR-C in left and right atria. Nevertheless, cANF effectively prevented left atrial fibrosis suggesting that there are sufficient levels of NPR-C in the left atrium to mediate some protective effects. As such, additional studies will be required to determine the basis for the differential effects of cANF on right and left atrial myocyte electrophysiology and fibrosis.

Our studies were performed in mouse models, which was essential for investigating the role of NPR-C in Ang II–mediated AF using NPR-C$^{-/-}$ mice. Because some of the effects we observed involve changes in AP duration and repolarizing K^+ currents, additional studies will be needed to validate these results in larger mammals and humans, where repolarization of the AP can involve K^+ channels, such as I_{Kr} and I_{Ks}, that are not present in the mouse heart. Nevertheless, I_{to} and I_{Kur}, which are affected by Ang II treatment, are important K^+ currents in humans, as well as mice. CV in the heart can be affected by heart rate,[8] and we have previously demonstrated that heart rate and sinoatrial node function are affected by Ang II.[32] Nevertheless, our data illustrate that the Ang II–induced changes in atrial CV in wild-type and NPR-C$^{-/-}$ mice were similar in sinus rhythm and during pacing at a fixed cycle length, suggesting that beating rate was not a major determinant of the changes in atrial conduction. Because of this observation, the effects of cANF on atrial CV were measured only in sinus rhythm. In addition to the targets investigated in our present study, atrial conduction and arrhythmogenesis could be affected by alterations in intercellular coupling via gap junctions. This was not investigated in our study; therefore, future investigations should consider the role of connexin expression and function and whether these are affected by NPs, in Ang II–mediated AF. In addition to NPR-C, It is important to recognize that NPR-A and NPR-B could also contribute to the effects of NPs in the atria, including in Ang II–mediated atrial dysfunction. Indeed, NPR-A and NPR-B affect ion channel function in the atria[17,31] and have also been shown to mediate some of the antifibrotic effects of NPs in the heart.[19,50] NPR-A and NPR-B have also been shown to play important roles in ventricular dysfunction in heart disease.[16,51,52] Accordingly, it will be important to assess the roles of NPR-A and NPR-B in Ang II–mediated AF and to determine how these receptors work in conjunction with NPR-C to regulate atrial remodeling and arrhythmogenesis.

In conclusion, our study demonstrates that NPR-C plays a critical role in the progression of Ang II–mediated AF and atrial dysfunction and identifies a novel approach of targeting NPR-C to prevent Ang II–mediated atrial remodeling. Current approaches to treating and preventing AF in conditions such as hypertension and heart failure, where pathological Ang II signaling is present, are limited. Our findings suggest that NPR-C may represent a new target for these conditions.

ARTICLE INFORMATION

Received September 5, 2018; accepted November 26, 2018.

The Data Supplement is available at https://www.ahajournals.org/doi/suppl/10.1161/CIRCEP.118.006863.

Correspondence

Robert A. Rose, PhD, Department of Cardiac Sciences, Libin Cardiovascular Institute of Alberta, Cumming School of Medicine, University of Calgary, GAC66, Health Research Innovation Centre, 3280 Hospital Dr NW, Calgary, Alberta T2N 4Z6, Canada. Email robert.rose@ucalgary.ca

Affiliations

Department of Cardiac Sciences, Libin Cardiovascular Institute of Alberta (H.J.J., M. Mackasey, Y.L., J.K., A.W.K., R.A.R.) and Department of Physiology and Pharmacology (H.J.J., M. Mackasey, Y.L., J.K., A.W.K., R.A.R.), Cumming School of Medicine, University of Calgary, Alberta. Department of Physiology and Biophysics, Dalhousie University, Halifax, Nova Scotia (M. Moghtadaei, E.E.E., S.A.R.). Department of Medicine, Schulich School of Medicine and Dentistry, Western University, London, Ontario, Canada (J.M.T.).

Sources of Funding

This work was supported by operating grants from the Canadian Institutes of Health Research to Dr Rose (MOP 93718, 142486). Dr Rose holds a New Investigator Award from the Heart and Stroke Foundation of Canada. Dr Jansen is the recipient of a Killam Postdoctoral Fellowship. M. Mackasey is the recipient of a Libin Cardiovascular Institute of Alberta Graduate Scholarship. Dr Liu is the recipient of a Libin Cardiovascular Institute/Cumming School of Medicine Postdoctoral Fellowship. Dr Egom held a Heart and Stroke Foundation of Canada Fellowship.

Disclosures

None.

REFERENCES

1. Schotten U, Verheule S, Kirchhof P, Goette A. Pathophysiological mechanisms of atrial fibrillation: a translational appraisal. *Physiol Rev*. 2011;91:265–325. doi: 10.1152/physrev.00031.2009
2. Heijman J, Voigt N, Nattel S, Dobrev D. Cellular and molecular electrophysiology of atrial fibrillation initiation, maintenance, and progression. *Circ Res*. 2014;114:1483–1499. doi: 10.1161/CIRCRESAHA.114.302226
3. Nattel S. Molecular and cellular mechanisms of atrial fibrosis in atrial fibrillation. *JACC Clin Electrophysiol*. 2017;3:425–435.
4. Khatib R, Joseph P, Briel M, Yusuf S, Healey J. Blockade of the renin-angiotensin-aldosterone system (raas) for primary prevention of non-valvular atrial fibrillation: a systematic review and meta analysis of randomized controlled trials. *Int J Cardiol*. 2013;165:17–24.
5. Purohit A, Rokita AG, Guan X, Chen B, Koval OM, Voigt N, Neef S, Sowa T, Gao Z, Luczak ED, Stefansdottir H, Behunin AC, Li N, El-Accaoui RN, Yang B, Swaminathan PD, Weiss RM, Wehrens XH, Song LS, Dobrev D, Maier LS, Anderson ME. Oxidized ca2+/calmodulin-dependent protein kinase II triggers atrial fibrillation. *Circulation*. 2013;128:1748–1757.
6. Jalife J. Mechanisms of persistent atrial fibrillation. *Curr Opin Cardiol*. 2014;29:20–27.
7. Bartos DC, Grandi E, Ripplinger CM. Ion channels in the heart. *Compr Physiol*. 2015;5:1423–1464. doi: 10.1002/cphy.c140069
8. Kléber AG, Rudy Y. Basic mechanisms of cardiac impulse propagation and associated arrhythmias. *Physiol Rev*. 2004;84:431–488. doi: 10.1152/physrev.00025.2003
9. Zhang Z, He Y, Tuteja D, Xu D, Timofeyev V, Zhang Q, Glatter KA, Xu Y, Shin HS, Low R, Chiamvimonvat N. Functional roles of Cav1.3(alpha1D) calcium channels in atria: insights gained from gene-targeted null mutant mice. *Circulation*. 2005;112:1936–1944. doi: 10.1161/CIRCULATIONAHA.105.540070

10. Nerbonne JM, Kass RS. Molecular physiology of cardiac repolarization. *Physiol Rev*. 2005;85:1205–1253. doi: 10.1152/physrev.00002.2005
11. Nattel S. New ideas about atrial fibrillation 50 years on. *Nature*. 2002;415:219–226. doi: 10.1038/415219a
12. Jalife J, Kaur K. Atrial remodeling, fibrosis, and atrial fibrillation. *Trends Cardiovasc Med*. 2015;25:475–484. doi: 10.1016/j.tcm.2014.12.015
13. Miragoli M, Glukhov AV. Atrial fibrillation and fibrosis: beyond the cardiomyocyte centric view. *Biomed Res Int*. 2015;2015:798768.
14. Takawale A, Sakamuri SS, Kassiri Z. Extracellular matrix communication and turnover in cardiac physiology and pathology. *Compr Physiol*. 2015;5:687–719. doi: 10.1002/cphy.c140045
15. Fan D, Takawale A, Lee J, Kassiri Z. Cardiac fibroblasts, fibrosis and extracellular matrix remodeling in heart disease. *Fibrogenesis Tissue Repair*. 2012;5:15. doi: 10.1186/1755-1536-5-15
16. Potter LR, Abbey-Hosch S, Dickey DM. Natriuretic peptides, their receptors, and cyclic guanosine monophosphate-dependent signaling functions. *Endocr Rev*. 2006;27:47–72. doi: 10.1210/er.2005-0014
17. Moghtadaei M, Polina I, Rose RA. Electrophysiological effects of natriuretic peptides in the heart are mediated by multiple receptor subtypes. *Prog Biophys Mol Biol*. 2016;120:37–49. doi: 10.1016/j.pbiomolbio.2015.12.001
18. Anand-Srivastava MB, Trachte GJ. Atrial natriuretic factor receptors and signal transduction mechanisms. *Pharmacol Rev*. 1993;45:455–497.
19. Rose RA, Giles WR. Natriuretic peptide C receptor signalling in the heart and vasculature. *J Physiol*. 2008;586:353–366. doi: 10.1113/jphysiol.2007.144253
20. Egom EE, Vella K, Hua R, Jansen HJ, Moghtadaei M, Polina I, Bogachev O, Hurnik R, Mackasey M, Rafferty S, Ray G, Rose RA. Impaired sinoatrial node function and increased susceptibility to atrial fibrillation in mice lacking natriuretic peptide receptor C. *J Physiol*. 2015;593:1127–1146. doi: 10.1113/jphysiol.2014.283135
21. Hua R, MacLeod SL, Polina I, Moghtadaei M, Jansen HJ, Bogachev O, O'Blenes SB, Sapp JL, Legare JF, Rose RA. Effects of wild-type and mutant forms of atrial natriuretic peptide on atrial electrophysiology and arrhythmogenesis. *Circ Arrhythm Electrophysiol*. 2015;8:1240–1254. doi: 10.1161/CIRCEP.115.002896
22. Azer J, Hua R, Vella K, Rose RA. Natriuretic peptides regulate heart rate and sinoatrial node function by activating multiple natriuretic peptide receptors. *J Mol Cell Cardiol*. 2012;53:715–724. doi: 10.1016/j.yjmcc.2012.08.020
23. Pagano M, Anand-Srivastava MB. Cytoplasmic domain of natriuretic peptide receptor C constitutes Gi activator sequences that inhibit adenylyl cyclase activity. *J Biol Chem*. 2001;276:22064–22070. doi: 10.1074/jbc.M101587200
24. Li Y, Sarkar O, Brochu M, Anand-Srivastava MB. Natriuretic peptide receptor-C attenuates hypertension in spontaneously hypertensive rats: role of nitroxidative stress and Gi proteins. *Hypertension*. 2014;63:846–855. doi: 10.1161/HYPERTENSIONAHA.113.01772
25. Jansen HJ, Moghtadaei M, Mackasey M, Rafferty SA, Bogachev O, Sapp JL, Howlett SE, Rose RA. Atrial structure, function and arrhythmogenesis in aged and frail mice. *Sci Rep*. 2017;7:44336. doi: 10.1038/srep44336
26. Tuomi JM, Chidiac P, Jones DL. Evidence for enhanced M3 muscarinic receptor function and sensitivity to atrial arrhythmia in the RGS2-deficient mouse. *Am J Physiol Heart Circ Physiol*. 2010;298:H554–H561. doi: 10.1152/ajpheart.00779.2009
27. Azer J, Hua R, Krishnaswamy PS, Rose RA. Effects of natriuretic peptides on electrical conduction in the sinoatrial node and atrial myocardium of the heart. *J Physiol*. 2014;592:1025–1045. doi: 10.1113/jphysiol.2013.265405
28. Krishnaswamy PS, Egom EE, Moghtadaei M, Jansen HJ, Azer J, Bogachev O, Mackasey M, Robbins C, Rose RA. Altered parasympathetic nervous system regulation of the sinoatrial node in Akita diabetic mice. *J Mol Cell Cardiol*. 2015;82:125–135. doi: 10.1016/j.yjmcc.2015.02.024
29. Moghtadaei M, Jansen HJ, Mackasey M, Rafferty SA, Bogachev O, Sapp JL, Howlett SE, Rose RA. The impacts of age and frailty on heart rate and sinoatrial node function. *J Physiol*. 2016;594:7105–7126. doi: 10.1113/JP272979
30. Jansen HJ, Mackasey M, Moghtadaei M, Belke DD, Egom EE, Tuomi JM, Rafferty SA, Kirkby AW, Rose RA. Distinct patterns of atrial electrical and structural remodeling in angiotensin II mediated atrial fibrillation. *J Mol Cell Cardiol*. 2018;124:12–25. doi: 10.1016/j.yjmcc.2018.09.011
31. Springer J, Azer J, Hua R, Robbins C, Adamczyk A, McBoyle S, Bissell MB, Rose RA. The natriuretic peptides BNP and CNP increase heart rate and electrical conduction by stimulating ionic currents in the sinoatrial node and atrial myocardium following activation of guanylyl cyclase-linked natriuretic peptide receptors. *J Mol Cell Cardiol*. 2012;52:1122–1134. doi: 10.1016/j.yjmcc.2012.01.018
32. Mackasey M, Egom EE, Jansen HJ, Hua R, Moghtadaei M, Liu Y, Kaur J, McRae M, Bogachev O, Rafferty S, Ray G, Kirkby AW, Rose RA. Natriuretic peptide receptor C (NPR-C) protects against angiotensin II mediated sinoatrial disease in mice. *JACC Basic Transl Sci*. 2018;3:824–833. doi: 10.1016/j.jacbts.2018.08.004
33. Lomax AE, Kondo CS, Giles WR. Comparison of time- and voltage-dependent K+ currents in myocytes from left and right atria of adult mice. *Am J Physiol Heart Circ Physiol*. 2003;285:H1837–H1848. doi: 10.1152/ajpheart.00386.2003
34. Kuo HC, Cheng CF, Clark RB, Lin JJ, Lin JL, Hoshijima M, Nguyên-Trân VT, Gu Y, Ikeda Y, Chu PH, Ross J, Giles WR, Chien KR. A defect in the Kv channel-interacting protein 2 (KChIP2) gene leads to a complete loss of I(to) and confers susceptibility to ventricular tachycardia. *Cell*. 2001;107:801–813.
35. Fiset C, Clark RB, Larsen TS, Giles WR. A rapidly activating sustained K+ current modulates repolarization and excitation-contraction coupling in adult mouse ventricle. *J Physiol*. 1997;504(pt 3):557–563.
36. Leask A. Potential therapeutic targets for cardiac fibrosis: TGFbeta, angiotensin, endothelin, CCN2, and PDGF, partners in fibroblast activation. *Circ Res*. 2010;106:1675–1680. doi: 10.1161/CIRCRESAHA.110.217737
37. Leask A. Getting to the heart of the matter: new insights into cardiac fibrosis. *Circ Res*. 2015;116:1269–1276. doi: 10.1161/CIRCRESAHA.116.305381
38. Takawale A, Zhang P, Patel VB, Wang X, Oudit G, Kassiri Z. Tissue inhibitor of matrix metalloproteinase-1 promotes myocardial fibrosis by mediating CD63-integrin β1 interaction. *Hypertension*. 2017;69:1092–1103. doi: 10.1161/HYPERTENSIONAHA.117.09045
39. Sopel MJ, Rosin NL, Lee TD, Légaré JF. Myocardial fibrosis in response to Angiotensin II is preceded by the recruitment of mesenchymal progenitor cells. *Lab Invest*. 2011;91:565–578. doi: 10.1038/labinvest.2010.190
40. Li J, Wang S, Bai J, Yang XL, Zhang YL, Che YL, Li HH, Yang YZ. Novel role for the immunoproteasome subunit PSMB10 in angiotensin II-induced atrial fibrillation in mice. *Hypertension*. 2018;71:866–876. doi: 10.1161/HYPERTENSIONAHA.117.10390
41. Fukui A, Takahashi N, Nakada C, Masaki T, Kume O, Shinohara T, Teshima Y, Hara M, Saikawa T. Role of leptin signaling in the pathogenesis of angiotensin II-mediated atrial fibrosis and fibrillation. *Circ Arrhythm Electrophysiol*. 2013;6:402–409. doi: 10.1161/CIRCEP.111.000104
42. Dobrzynski H, Boyett MR, Anderson RH. New insights into pacemaker activity: promoting understanding of sick sinus syndrome. *Circulation*. 2007;115:1921–1932. doi: 10.1161/CIRCULATIONAHA.106.616011
43. Gomes JA, Kang PS, Matheson M, Gough WB Jr, El-Sherif N. Coexistence of sick sinus rhythm and atrial flutter-fibrillation. *Circulation*. 1981;63:80–86.
44. Leask A, Abraham DJ. TGF-beta signaling and the fibrotic response. *FASEB J*. 2004;18:816–827. doi: 10.1096/fj.03-1273rev
45. Kunamalla A, Ng J, Parini V, Yoo S, McGee KA, Tomson TT, Gordon D, Thorp EB, Lomasney J, Zhang Q, Shah S, Browne S, Knight BP, Passman R, Goldberger JJ, Aistrup G, Arora R. Constitutive expression of a dominant-negative TGF-β type II receptor in the posterior left atrium leads to beneficial remodeling of atrial fibrillation substrate. *Circ Res*. 2016;119:69–82. doi: 10.1161/CIRCRESAHA.115.307878
46. Fan D, Takawale A, Basu R, Patel V, Lee J, Kandalam V, Wang X, Oudit GY, Kassiri Z. Differential role of TIMP2 and TIMP3 in cardiac hypertrophy, fibrosis, and diastolic dysfunction. *Cardiovasc Res*. 2014;103:268–280. doi: 10.1093/cvr/cvu072
47. Yeh YH, Kuo CT, Lee YS, Lin YM, Nattel S, Tsai FC, Chen WJ. Region-specific gene expression profiles in the left atria of patients with valvular atrial fibrillation. *Heart Rhythm*. 2013;10:383–391. doi: 10.1016/j.hrthm.2012.11.013
48. Santangeli P, Zado ES, Hutchinson MD, Riley MP, Lin D, Frankel DS, Supple GE, Garcia FC, Dixit S, Callans DJ, Marchlinski FE. Prevalence and distribution of focal triggers in persistent and long-standing persistent atrial fibrillation. *Heart Rhythm*. 2016;13:374–382. doi: 10.1016/j.hrthm.2015.10.023
49. Haïssaguerre M, Wright M, Hocini M, Jaïs P. The substrate maintaining persistent atrial fibrillation. *Circ Arrhythm Electrophysiol*. 2008;1:2–5. doi: 10.1161/CIRCEP.108.764233
50. Jansen HJ, Rose RA. Natriuretic peptides: critical regulators of cardiac fibroblasts and the extracellular matrix in the heart. In: Dixon IM, Wigle JT, eds. *Cardiac Fibrosis and Heart Failure: Cause or Effect*. New York, NY: Springer International Publishing. 2015:383–404.
51. Kuhn M. Molecular physiology of membrane guanylyl cyclase receptors. *Physiol Rev*. 2016;96:751–804. doi: 10.1152/physrev.00022.2015
52. Kuhn M. Function and dysfunction of mammalian membrane guanylyl cyclase receptors: lessons from genetic mouse models and implications for human diseases. *Handb Exp Pharmacol*. 2009;191:47–69.

SUPPLEMENTAL MATERIAL

Supplemental Methods

Mice

This study used wildtype (C57BL/6; Charles River Laboratories) and NPR-C$^{-/-}$ mice. NPR-C$^{-/-}$ mice were initially obtained from Jackson Laboratory (strain: B6;C-*Npr3lgj*/J) then backcrossed with C57BL/6 mice for more than 15 generations in the animal care facility before being used for experiments.

Mice were implanted with subcutaneous miniosmotic pumps (Alzet model 1004) to allow for the continuous delivery of saline, Ang II (3 mg/kg/day; Bachem H-1705), or Ang II with cANF (0.07 or 0.14 mg/kg/day; Bachem H-3134) for 3 days or 3 weeks as indicated in the manuscript. Saline was used as a vehicle control. To insert the pumps mice were anaesthetized with 2% isoflurane inhalation and pumps were inserted subcutaneously via a mid-scapular incision. Mice then were administered a 5 mg/kg of the analgesic ketoprofen.

In vivo electrophysiology

A 1.2 French octapolar electrophysiology catheter was used for intracardiac pacing experiments using the neuro/Craft StimPulse Stimulator as we have described previously.[1,2] Inducibility of AF was studied using burst pacing in the right atrium.[1,2] We used 3 trains of 2 s burst pacing as follows: the first 2 s burst was given at a cycle length of 40 ms with a pulse duration of 5 ms. Following 3 min of stabilization a second 2 s burst was applied at a cycle length 20 ms with a pulse duration of 5 ms. After another 3 min of stabilization the final 2 s burst was given at a cycle length of 20 ms with a pulse duration of 10 ms. AF was defined as a rapid and irregular atrial rhythm (fibrillatory baseline in the ECG) combined with irregular RR intervals that lasted at least 1 s on the surface ECG. ERP measurements were determined using a S1-S2 protocol where an 8 stimulus drive train (S1) at a fixed cycle length of 100 ms was delivered followed by

an extra stimulus (S2) at a progressively shorter cycle length. ERPs were defined as the shortest S1-S2 interval that allowed for capture of the region of interest. This was defined as the P wave for AERP measurements and a dropped QRS complex for AVERP measurements. Temperature was measured using a rectal probe and maintained at 37°C using a heating pad. All ECG data were acquired using a Gould ACQ-7700 amplifier and Ponemah Physiology Platform software (Data Sciences International) as we have described previously.[1,2]

High resolution optical mapping

We used high resolution optical mapping to study patterns of electrical conduction in the mouse atria as we have done previously.[2-4] To isolate our atrial preparation mice were administered a 0.2 ml intraperitoneal injection of heparin (1000 IU/ml) to prevent blood clotting and were then anesthetized by isoflurane inhalation and sacrificed by cervical dislocation. Hearts were excised into Krebs solution (35°C) containing (in mM): 118 NaCl, 4.7 KCl, 1.2 KH_2PO_4, 12.2 $MgSO_4$, 1 $CaCl_2$, 25 $NaHCO_3$, 11 glucose and bubbled with 95% O_2/5% CO_2 to maintain a pH of 7.4. The atria were dissected away from the ventricles and pinned in a dish with the epicardial surface facing upwards (towards the imaging equipment). The superior and inferior vena cavae were cut open so that the crista terminalis could be visualized and the preparation could be pinned out flat.

The atrial preparation was superfused continuously with Krebs solution (35°C) bubbled with 95% O_2/5% CO_2 and allowed to equilibrate for at least 30 min. During this time the preparation was treated with the voltage sensitive dye di-4-ANEPPS (10 µM) for ~15 min and blebbistatin (10 µM) was added to the superfusate to suppress contractile activity and prevent motion artifacts.[5,6] Experiments were performed in sinus rhythm so that the cycle length (i.e. beating rate) of the atrial preparation was free to change as well as in atrial preparations paced at a fixed cycle length of 125 ms in order to study electrical conduction independently of

changes in cycle length. The pacing electrode was placed near the opening of the superior vena cava.

Di-4-ANEPPS loaded atrial preparations were illuminated with light at a wavelength of 520 – 570 nM using an EXFO X-cite fluorescent light source (Lumen Dynamics). Emitted light (590 – 640 nM) was captured using a high speed EMCCD camera (Evolve 128, Photometrics). Data were captured from an optical field of view of 8 x 8 mm^2 at a frame rate of ~900 frames/s using Metamorph software (Molecular Devices). The spatial resolution was 67 x 67 μM for each pixel. Magnification was constant in all experiments and no pixel binning was used.

All optical data were analyzed using custom software written in Matlab. Pseudocolor electrical activation maps were generated from measurements of activation time at individual pixels as defined by assessment of dF/dt_{max} and background fluorescence was subtracted in all cases. Local conduction velocity (CV) was quantified specifically in the right atrial myocardium (within the right atrial appendage) and the left atrial myocardium (within the left atrial appendage) using an established approach previously described.[3,7,8] Briefly, activation times at each pixel from a 7 x 7 pixel array were determined and fit to a plane using the least squares fit method. The direction on this plane that is increasing the fastest represents the direction that is perpendicular to the wavefront of electrical propagation and the maximum slope represents the inverse of the speed of conduction in that direction. With a spatial resolution of 67 x 67 μM per pixel, the area of the 7 x 7 pixel array was 469 x 469 μM. This approach allows us to compute the maximum local CV vectors in the atrial region of interest. Optical APs were assessed by measuring the change in fluorescence as a function of time at individual pixels within the right and left atria as we have done previously.[2,9]

Isolation of mouse atrial myocytes

The procedures for isolating mouse atrial myocytes have been described previously.[10,11] Mice were administered a 0.2 ml intraperitoneal injection of heparin (1000 IU/ml) to prevent

blood clotting. Briefly, mice were anaesthetized using isoflurane inhalation and then sacrificed by cervical dislocation. The heart was excised into Tyrode's solution (35ºC) consisting of (in mM): 140 NaCl, 5.4 KCl, 1.2 KH_2PO_4, 1.0 $MgCl_2$, 1.8 $CaCl_2$, 5.55 glucose, and 5 HEPES, with pH adjusted to 7.4 with NaOH. Heparin was added to the Tyrode's solution to prevent blood clotting. The right or left atrial appendage was dissected from the heart, cut into strips and then equilibrated and washed in a 'low Ca^{2+}, Mg^{2+} free' solution containing (in mM): 140 NaCl, 5.4 KCl, 1.2 KH_2PO_4, 0.2 $CaCl_2$, 50 taurine, 18.5 glucose, 5 HEPES and 1 mg/ml bovine serum albumin (BSA), with pH adjusted to 6.9 with NaOH. Next, atrial tissue strips were enzymatically digested for 30 min in 5 ml of 'low Ca^{2+}, Mg^{2+} free' solution that contained collagenase (type II, Worthington Biochemical Corporation), elastase (Worthington Biochemical Corporation) and protease (type XIV, Sigma Chemical Company). Next, the tissue was transferred to 2.5 ml of modified KB solution containing (in mM): 100 potassium glutamate, 10 potassium aspartate, 25 KCl, 10 KH_2PO_4, 2 $MgSO_4$, 20 taurine, 5 creatine, 0.5 EGTA, 20 glucose, 5 HEPES, and 0.1% BSA, with pH adjusted to 7.2 with KOH. Digested tissue strips were mechanically agitated using a wide-bore pipette. This procedure yielded individual right or left atrial myocytes that were stored in KB solution at room temperature and used for electrophysiology experiments within 6 hours of isolation.

Solutions and electrophysiological protocols

Stimulated action potentials (APs) were recorded using either the perforated patch-clamp technique or the whole cell patch-clamp technique. There were no differences in AP parameters between perforated and whole cell configurations. Stimulated APs were superfused with normal Tyrode's solution (22 – 23ºC) containing (in mM): 140 NaCl, 5 KCl, 1 $MgCl_2$, 1 $CaCl_2$, 10 HEPES, and 5 glucose, with pH adjusted to 7.4 with NaOH. The pipette filling solution contained (in mM): 135 KCl, 0.1 $CaCl_2$, 1 $MgCl_2$, 5 NaCl, 10 EGTA, 4 Mg-ATP, 6.6 Na-phosphocreatine, 0.3 Na-GTP and 10 HEPES, with pH adjusted to 7.2 with KOH. Amphotericin

B (200 µg/ml) was added to this pipette solution to record APs with the perforated patch clamp technique.

I_{Na} was recorded in atrial myocytes using a modified Tyrode's solution containing (in mM): 130 CsCl, 5 NaCl, 5.4 TEA-Cl, 1 $MgCl_2$, 1 $CaCl_2$, 10 HEPES, 5.5 glucose and adjusted to pH 7.4 with CsOH. Nifedipine (10 µM) was added to block $I_{Ca,L}$. The pipette solution contained (in mM): 5 NaCl, 130 CsCl, 1 $MgCl_2$, 0.2 $CaCl_2$, 10 HEPES, 5 BAPTA, 5 Mg-ATP, 0.3 Na-GTP and adjusted to pH 7.2 with CsOH. The voltage clamp protocol used to record I_{Na} was a series of 50 ms voltage clamp steps from -100 to +50 mV in 10 mV increments from a holding potential of -120 mV.

I_{Na} activation kinetics were determined by calculating chord conductance (G) with the equation $G=I/(V_m-E_{rev})$, where V_m represents the depolarizing voltages and E_{rev} is the reversal potential measured from the current-voltage relationships of I_{Na}. Maximum conductance (G_{max}) and $V_{1/2}$ of activation for $I_{Ca,L}$ and I_{Na} were determined using the following function: $G=[(V_m-V_{rev})][G_{max}][-1/[(1+\exp((V_m-V_{1/2})/k))+1]]$.

Potassium currents (I_K) were recorded in the whole cell configuration of the patch clamp technique using the same Tyrode's solution and pipette solutions used to record APs. To record total potassium currents (no pre-pulse), cells were held at -80 mV then I_K was recorded using a series of voltage clamp steps (500 ms duration) between -120 and +80 mV in 10 mV increments. To record potassium currents with an inactivating pre-pulse (to inactivate I_{to}), cells were given a 200 ms pre-pulse to -40 mV immediately followed by 500 ms voltage clamp steps from -120 to +80 mV from a holding potential of -80 mV. For these recordings with and without a pre-pulse, I_K was measured at the peak current for each voltage step. I_{to} was calculated as the difference current between the recordings with and without a pre-pulse.[12,13]

I_{Kur}, as carried by $K_V1.5$ channels, was measured as the component of I_K sensitive to 4-aminopyradine (4-AP; 100 µM).[12,14] The voltage clamp protocol for measuring I_{Kur} included a

pre-pulse to -40 mV for 200 ms to inactivate I_{to} immediately followed by a 500 ms step to +30 mV before returning to a holding potential of -80 mV. Peak currents at baseline, in the presence of 4-AP, and after washout were measured.

Micropipettes were pulled from borosilicate glass (with filament, 1.5 mm OD, 0.75 mm ID, Sutter Instrument Company) using a Flaming/Brown pipette puller (model p-87, Sutter Instrument Company). The resistance of these pipettes was 4 – 8 MΩ when filled with pipette solution. Micropipettes were positioned using a micromanipulator (Burleigh PCS-5000 system) mounted on the stage of an inverted microscope (Olympus IX71). Seal resistance was 2 – 15 GΩ and access resistances were 5 – 15 MΩ following rupture of the sarcolemma. Series resistance compensation to 85% using an Axopatch 200B amplifier (Molecular Devices). For perforated patch clamp experiments access resistance was monitored for the development of capacitative transients upon sealing to the cell membrane with Amphotericin B in the pipette. Typically, access resistance became less than 30 MΩ within 5 min of sealing onto the cell, which was sufficient for recording stimulated APs in current clamp mode. Data were digitized using a Digidata 1440 and pCLAMP 10 software (Molecular Devices) and stored on computer for analysis. No junction potential corrections were applied in our analyses. All patch-clamp studies were conducted at room temperature.

Western blotting

Protein samples were extracted from the right or left atrial appendage. Tissue was cooled in liquid nitrogen, ground into a powder, and then incubated for 1 hour with ice-cold modified RIPA buffer that contained (in mM): 50 mM Tris, 150 mM NaCl, 25 mM sucrose, 1 mM EDTA, 1% Triton, 0,1% SDS. Protease inhibitor cocktail (Sigma-Aldrich) and 0.5 mM DTT (1,4-Dithiothreitol, Roche) were added to prevent protein degradation. Next, preparations were centrifuged for 10 min at 10 000 rpm at 4ºC and protein concentrations were measured using the Bio-Rad *DC*™ Protein Assay Kit II (Bio-Rad Laboratories). Protein samples (20 µg/lane)

were separated by 7.5% SDS-polyacrylamide gels (SDS-PAGE) and transferred onto a BioTrace™ NT Nitrocellulose Transfer Membrane (VWR). For KChIP2 western blot experiments, a protein concentration of 40 µg/lane was used and proteins were separated on a 15% SDS-PAGE gel. The membrane was blocked for 1 hour at room temperature with 1% casein in Tris-buffered saline (TBS; Bio-Rad Laboratories). Blots were incubated overnight at 4ºC with primary antibodies to PKCα (1:500, Cell Signaling Technology), NPR-A (1:500, Abcam), NPR-B (1:1000, Abcam), NPR-C (1:500, Abcam), or GAPDH (1:5000 Abcam), K_V4.2 (1:500, Alomone Labs), K_V4.3 (1:500, Alomone Labs), K_V1.5 (1:500, Alomone Labs), or KChIP2 (1:500, Alomone Labs). The western blot membranes were then washed 3 times in 1% TBST (TBS with 1% Tween 20 (Bio-Rad Laboratories)) before secondary antibody binding. In PKCα, K_V4.2, K_V4.3, K_V1.5, and KChIP2 experiments we used a fluorescent secondary approach and incubated the membrane with goat anti-rabbit IgG StarBright Blue 700 (1:2500, Bio-Rad Laboratories) and hFAB Rhodamine Anti-GAPDH IgG (1:3000, Bio-Rad Laboratories) for 1 hour at room temperature and then washed the membrane 3 times with 1% TBST before imaging. For NPR-A, NPR-B, and NPR-C experiments we used the ECL approach and incubated blots for 1 hour at room temperature with goat anti-rabbit IgG coupled to horseradish peroxidase (HRP; 1:2000, Abcam) for 1 hour at room temperature. The membrane was washed 3 times with 1% TBST before adding the ECL substrate (Bio-Rad) for 5 min prior to imaging. All western blot membranes were imaged using the ChemiDoc™ MP Imaging System (Bio-Rad Laboratories). Protein expression was normalized to GAPDH.

Quantitative PCR

Total RNA was isolated from right or left atrial appendages according to kit instructions using the PureZOL™ RNA Isolation Reagent and the Aurum™ Total RNA Fatty and Fibrous Tissue Kit (Bio-Rad Laboratories). RNA samples were eluted from the spin column in 40 µL elution buffer and both RNA yield and purity were assessed using a Nanodrop. All samples had

a A_{260}/A_{280} of over 2.0 and therefore were free of DNA contamination. We also assessed RNA integrity using the Experion RNA StdSens Analysis Kit (Bio-Rad Laboratories). cDNA (20 ng/µL) was synthesized using the iScript™ cDNA Synthesis Kit (Bio-Rad Laboratories). Reactions were performed in a Bio-Rad MyCycler thermal cycler using the following protocol: 5 min of priming at 25ºC followed by reverse transcription for 30 min at 42ºC then 5 min at 85ºC to inactivate reverse transcriptase.

All qPCR reactions were run in duplicate in 10 µL reactions that contained the following: 4 µL sample cDNA, 5.6 µL GoTaq® qPCR Master Mix (Promega), and 0.4 µL primers. Primers were reconstituted to a final concentration of 100 µM with nuclease free water and stored at -20ºC until use. Primers were diluted to 10 µM for qPCR reactions. RT-qPCR reactions were performed using the CFX386 Touch™ Real-Time PCR Detection System (Bio-Rad) using the following protocol: Taq polymerase was activated for 2 min at 95ºC followed by 39 cycles of denaturing for 15 s at 95ºC, annealing for 30 s at 60ºC, and extension for 30s at 72ºC. This was followed by melt curve analysis from 65-95ºC in 0.5ºC increments. Data were analyzed using the $2^{-\Delta\Delta C}{}_T$ method using the CFX Manager Software version 3.1 (Bio-Rad). Gene expression was normalized to GAPDH and β-actin. Primer sequences are provided in Supplemental Table 9.

Supplemental Figures

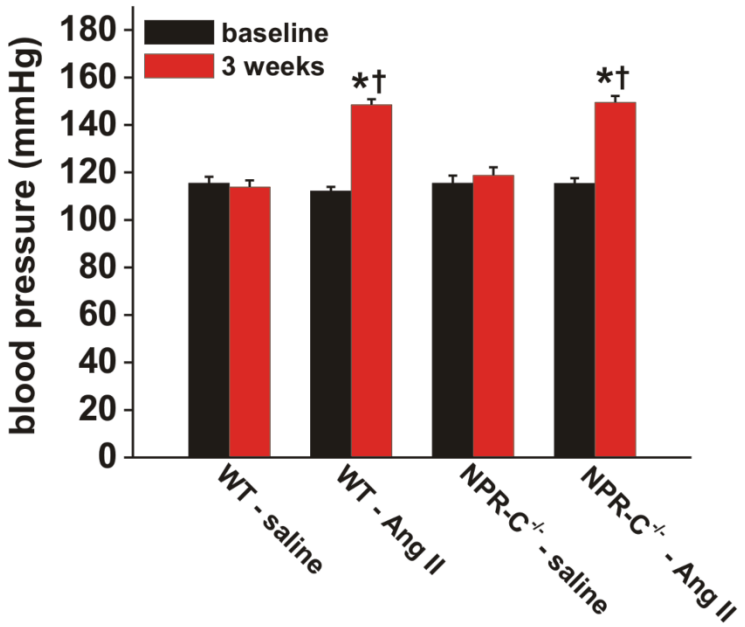

Supplemental Figure 1: Effects of Ang II on systolic blood pressure in wildtype and NPR-C$^{-/-}$ mice. Measurements were taken at baseline and following three weeks of treatment with Ang II. *P<0.05 vs. baseline within treatment group; $^{\dagger}P$<0.05 vs. saline at the 3 week time point. There were no differences (P=0.267) in systolic pressure at the 3 week time point between wildtype and NPR-C$^{-/-}$ mice. n=15 for WT/saline, 16 for WT/Ang II, 11 for NPR-C$^{-/-}$/saline and 11 for NPR-C$^{-/-}$/Ang II.

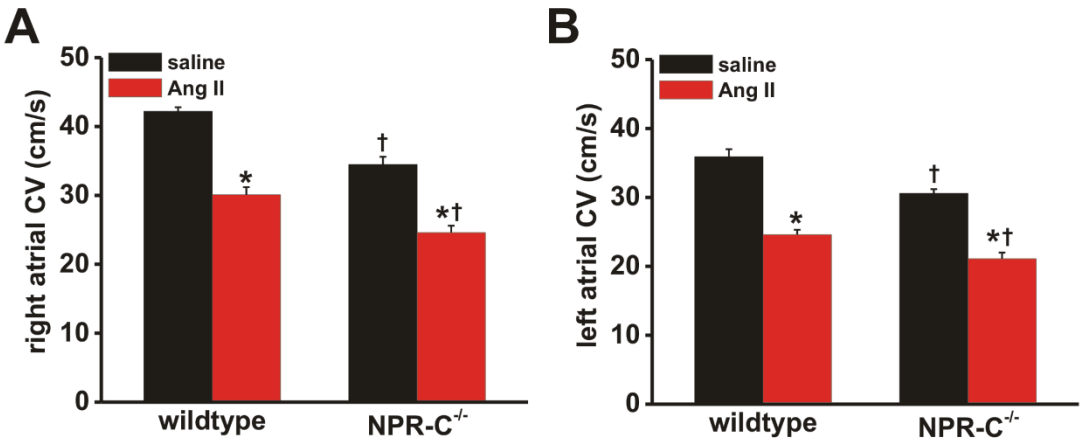

Supplemental Figure 2: Effects of Ang II on atrial conduction velocity in wildtype and NPR-C$^{-/-}$ mice in paced atrial preparations. Atrial preparations were paced a fixed cycle length of 125 ms. **A,** Summary of right atrial CV in wildtype and NPR-C$^{-/-}$ mice treated with saline or Ang II. **B,** Summary of left atrial CV in wildtype and NPR-C$^{-/-}$ mice treated with saline or Ang II. *P<0.05 vs. saline; $^{\dagger}P$<0.05 vs. wildtype by two-way ANOVA with Tukey's posthoc test; n=5 hearts for each group.

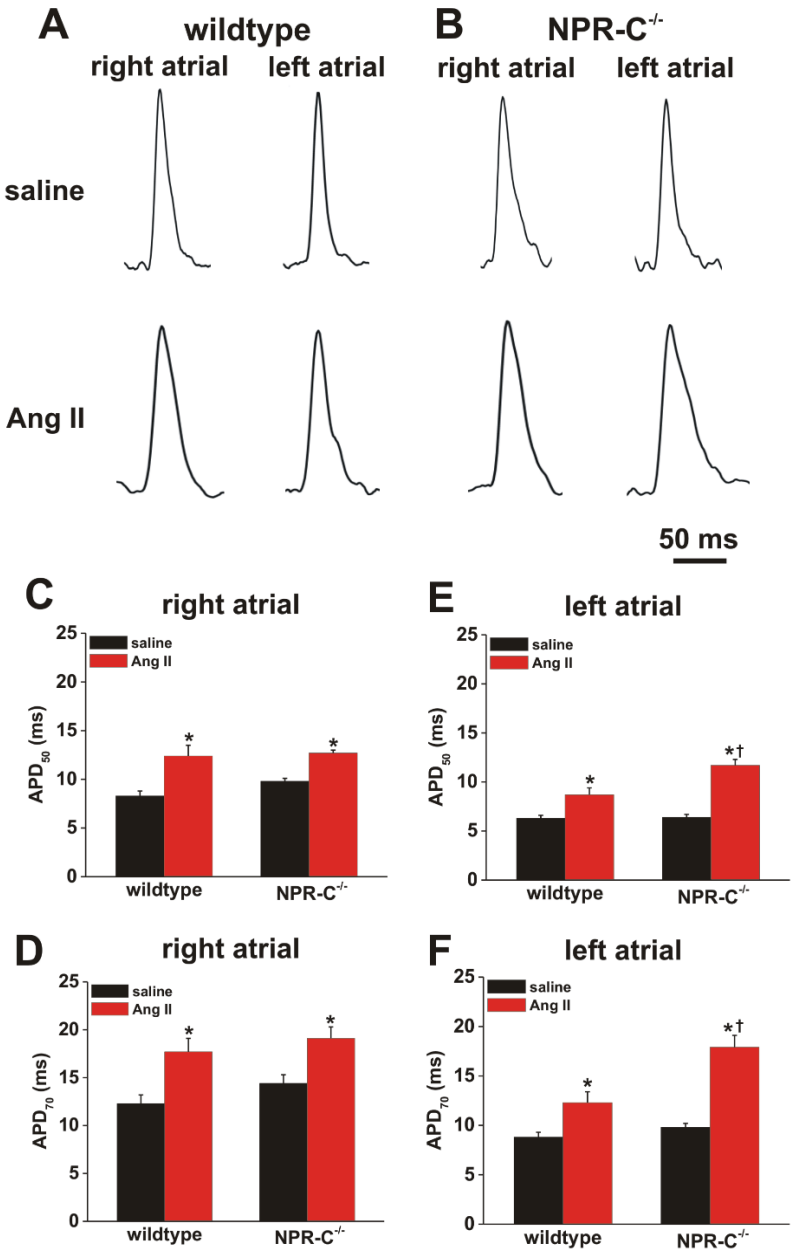

Supplemental Figure 3: Effects of Ang II on optical action potential duration in wildtype and NPR-C$^{-/-}$ mice. A, Representative optical APs in the right and left atria in wildtype mice treated with saline or Ang II. **B,** Representative optical APs in the right and left atria in NPR-C$^{-/-}$ mice treated with saline or Ang II. Summary data illustrate the effects of Ang II on APD_{50} in right (**C**) and left (**D**) atria as well as on APD_{70} in right (**E**) and left (**F**) atria in wildtype and NPR-C$^{-/-}$ mice. *P<0.05 vs. saline, $^{\dagger}P$<0.05 vs. wildtype by two-way ANOVA with Tukey's posthoc test; n=8 hearts for WT/saline, 8 for WT/Ang II, 5 for NPR-C$^{-/-}$/saline and 5 for NPR-C$^{-/-}$/Ang II.

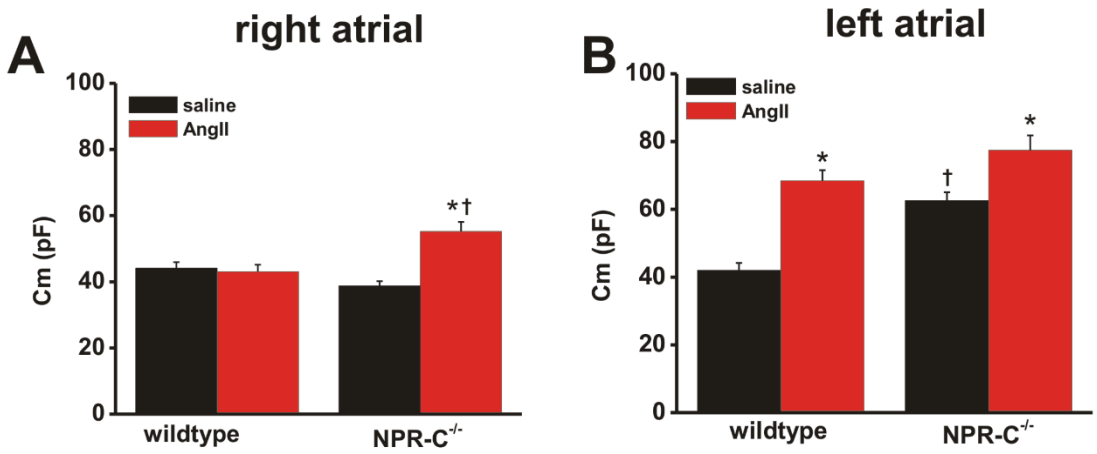

Supplemental Figure 4: Cell capacitance in right (A) and left (B) atrial myocytes from wildtype and NPR-C$^{-/-}$ mice treated with saline or Ang II. *P<0.05 vs. saline; †P<0.05 vs. wildtype, for the left atrium P=0.058 for NPR-C$^{-/-}$/Ang II vs. wildtype/Ang II by two-way ANOVA with Tukey's posthoc test; for right atrial myocytes n=29 for wildtype/saline, 28 for wildtype/Ang II, 35 for NPR-C$^{-/-}$/saline, and 43 for NPR-C$^{-/-}$/Ang II. For left atrial myocytes n=29 for wildtype/saline, 30 for wildtype/Ang II, 41 for NPR-C$^{-/-}$/saline, and 42 for NPR-C$^{-/-}$/Ang II

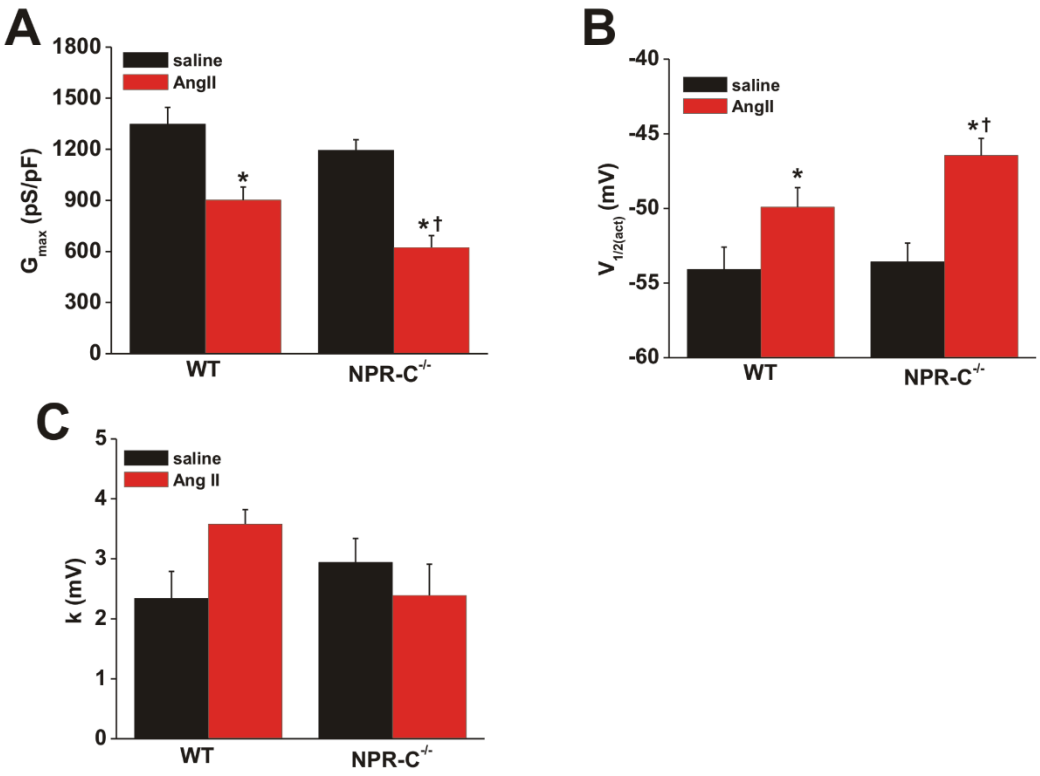

Supplemental Figure 5: I_{Na} activation kinetics in left atrial myocytes from wildtype and NPR-C$^{-/-}$ mice treated with saline or Ang II. Summary data for G_{max} (**A**), $V_{1/2(act)}$ (**B**) and k (**C**) are shown. *P<0.05 vs. saline; †P<0.05 vs. WT by two-way ANOVA with Tukey's posthoc test; n=9 for WT/saline, 10 for WT/Ang II, 9 for NPR-C$^{-/-}$/Ang II and 14 for NPR-C$^{-/-}$/Ang II.

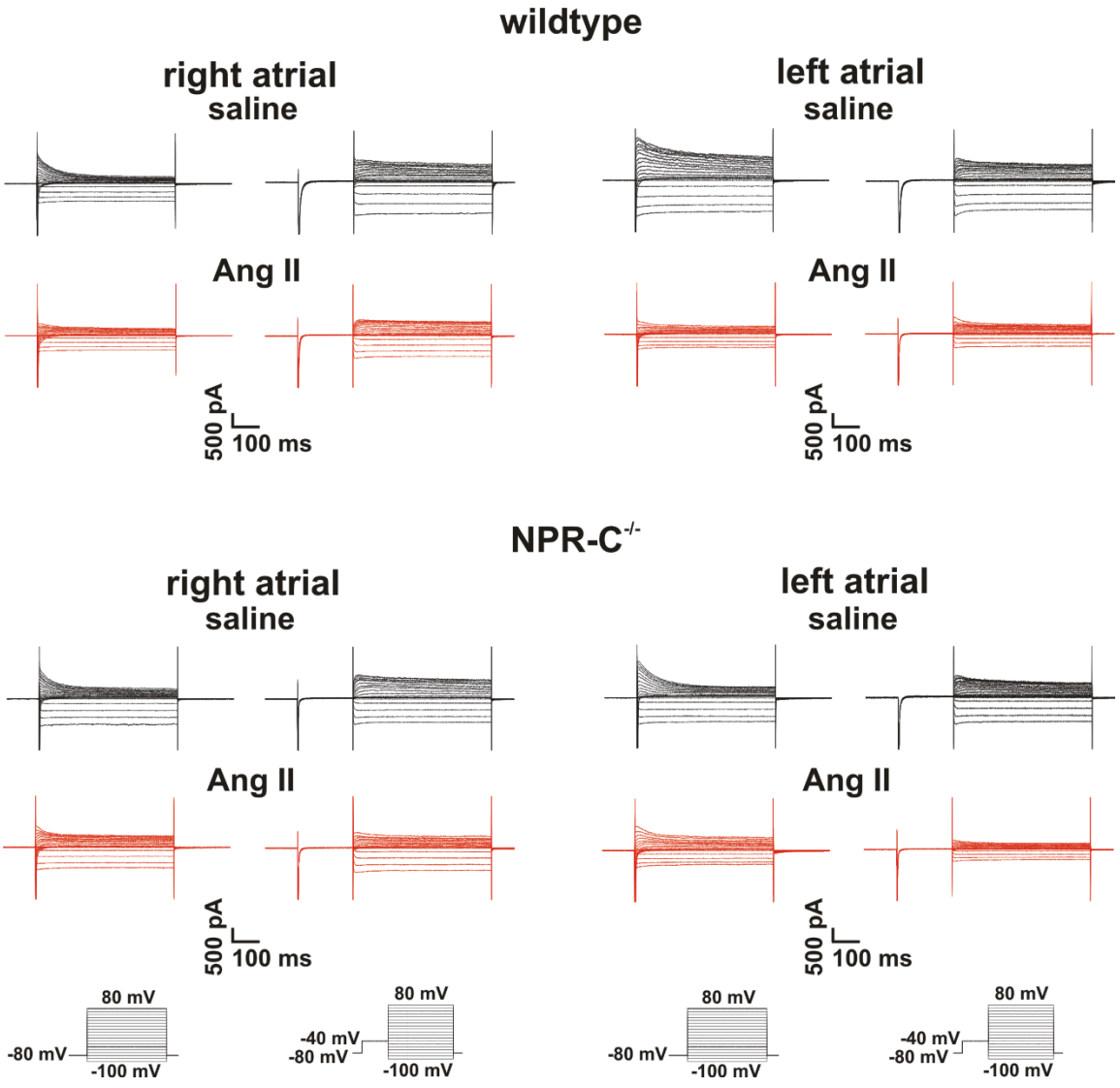

Supplemental Figure 6: Representative K^+ current recordings in right and left atrial myocytes isolated from wildtype and NPR-$C^{-/-}$ mice treated with saline or Ang II. Currents were recorded with and without a pre-pulse to -40 mV to inactivate I_{to}. Voltage clamp protocols are illustrated at the bottom of the figure. Summary data for these recordings are located in Figure 4 of the main paper.

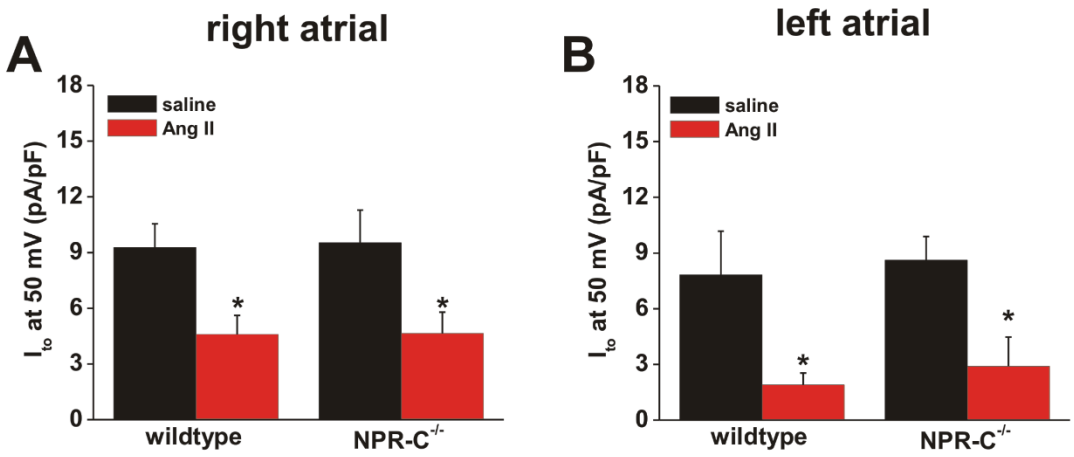

Supplemental Figure 7: Summary of I_{to} density at +50 mV in right (A) and left (B) atrial myocytes from wildtype and NPR-C$^{-/-}$ mice treated with saline or Ang II. **P*<0.05 vs. saline by two-way ANOVA with Tukey's posthoc test. There were no differences in I_{to} between wildtype and NPR-C$^{-/-}$ mice in right (*P*=0.804) or left (*P*=0.390) atrial myocytes; for right atrial myocytes *n*=29 for wildtype/saline, 16 for wildtype/Ang II, 16 for NPR-C$^{-/-}$/saline and 23 for NPR-C$^{-/-}$/Ang II; for left atrial myocytes *n*=12 for wildtype/saline, 20 for wildtype/Ang II, 17 for NPR-C$^{-/-}$/saline and 13 for NPR-C$^{-/-}$/Ang II.

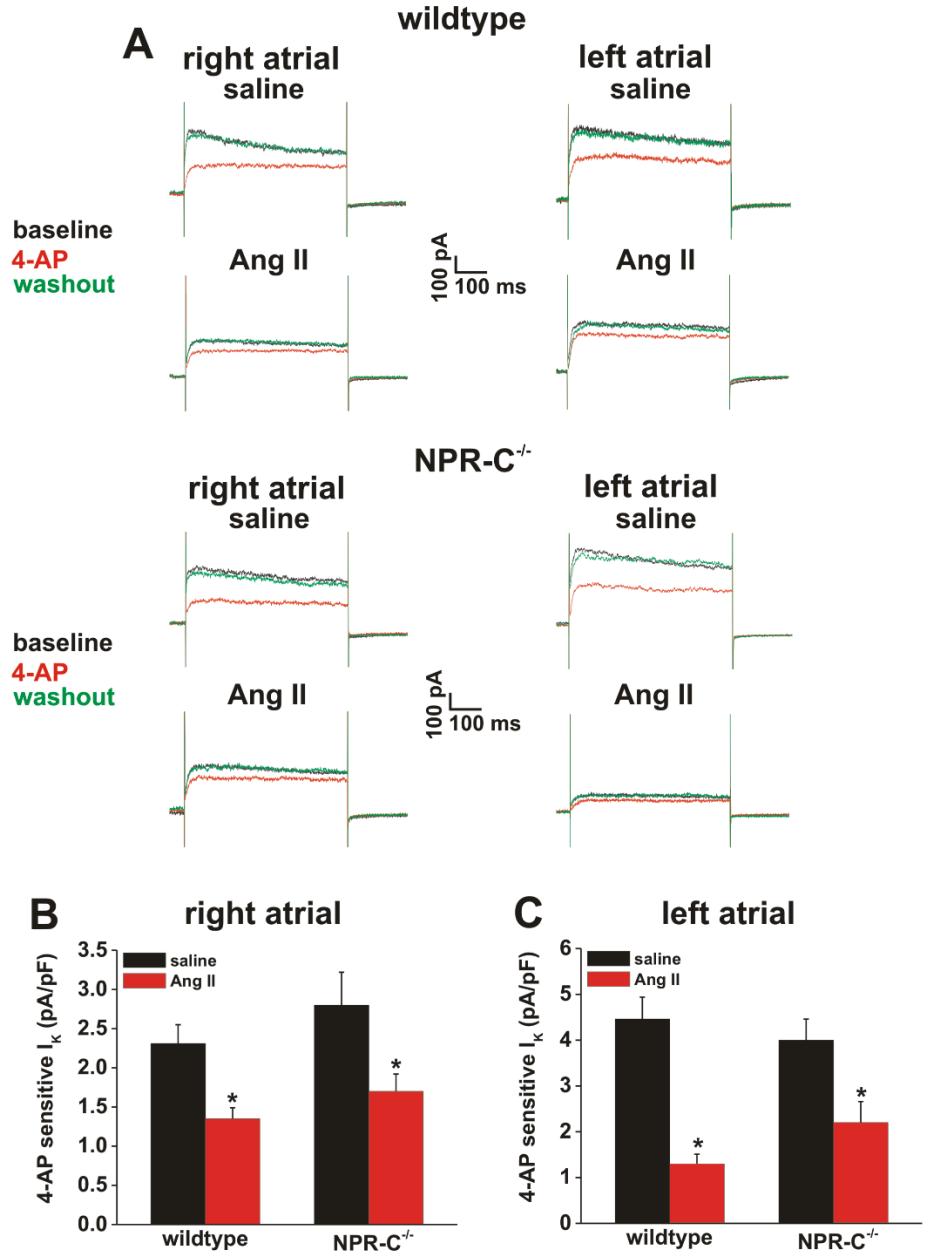

Supplemental Figure 8: Effects of Ang II on I_{Kur} in right and left atrial myocytes from wildtype and NPR-C$^{-/-}$ mice. A, Representative I_K recordings at +30 mV illustrating the effects of 4-AP (100 μM), which inhibits $K_V1.5$ mediated I_{Kur}, in right and left atrial myocytes from wildtype and NPR-C$^{-/-}$ mice treated with saline or Ang II. **B and C**, Summary of the effects of Ang II on the magnitude of the 4-AP sensitive I_K in right (**B**) and left (**C**) atrial myocytes in wildtype and NPR-C$^{-/-}$ mice. *P<0.05 vs. saline by two-way ANOVA with Tukey's posthoc test. There were no differences in 4-AP sensitive I_K between in right (P=0.119) or left (P=0.897) atrial myocytes from wildtype and NPR-C$^{-/-}$ mice; for right atrial myocytes n=19 for wildtype/saline, 13 for wildtype/Ang II, 12 for NPR-C$^{-/-}$/saline, and 13 for NPR-C$^{-/-}$/Ang II; for left atrial myocytes n=11 for wildtype/saline, 8 for wildtype/Ang II, 14 for NPR-C$^{-/-}$/saline, and 7 for NPR-C$^{-/-}$/Ang II.

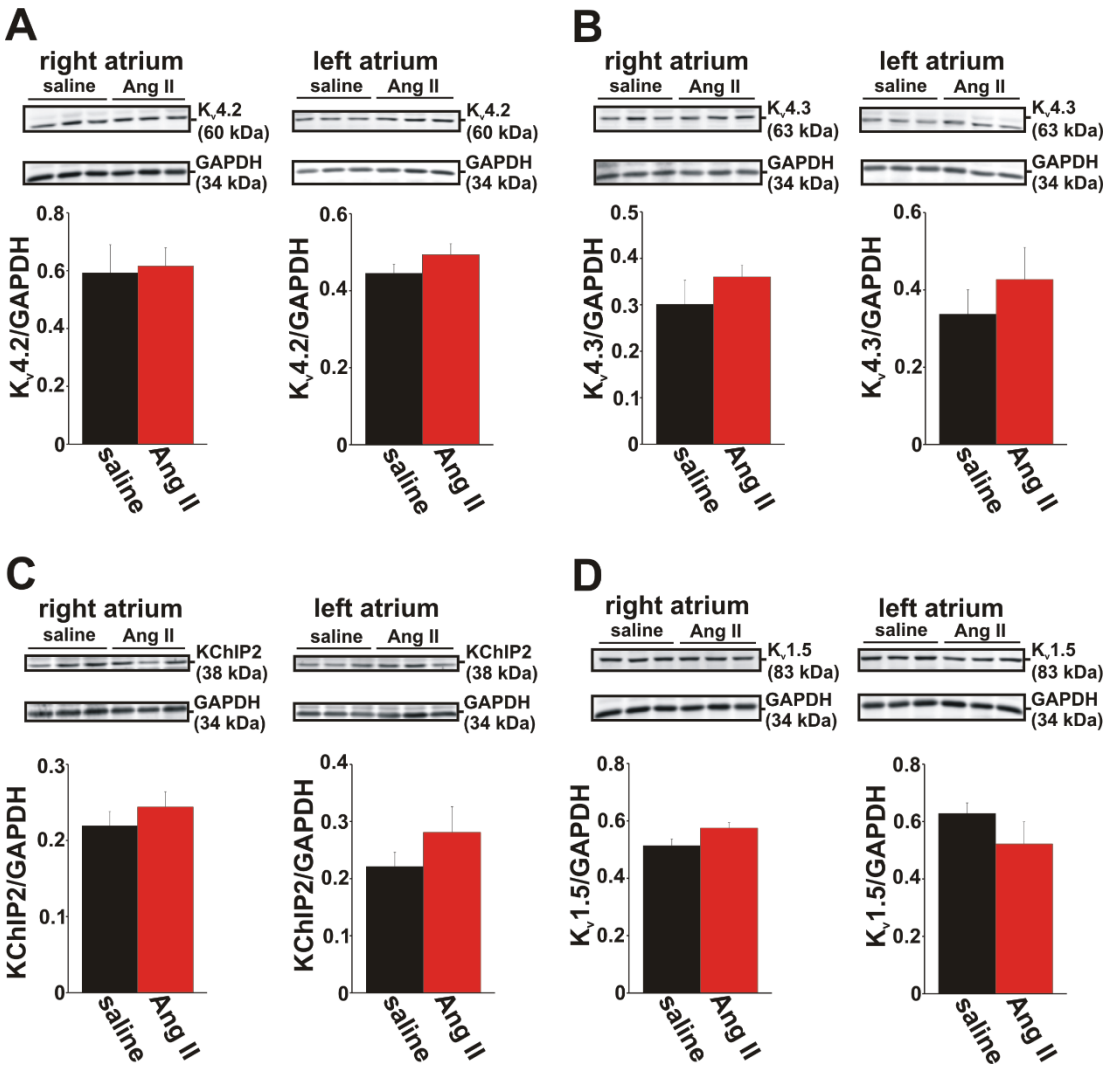

Supplemental Figure 9: Effects of Ang II on K^+ channel protein expression in NPR-C$^{-/-}$ mice. Representative Western blots and summary data are shown for the right and left atria for K_V4.2 (**A**), K_V4.3 (**B**), KChIP2 (**C**) and K_V1.5 (**D**). Ang II had no effects on protein expression of K_V4.2 in the right (*P*=0.842) or left (*P*=0.212) atria, K_V4.3 in the right (*P*=0.331) or left (*P*=0.405) atria, KChIP2 in the right (*P*=0.379) or left (*P*=0.276) atria or K_V1.5 in the right (*P*=0.07) or left (*P*=0.246) atria. Data analyzed by Student's *t*-test; *n*=6 hearts per group.

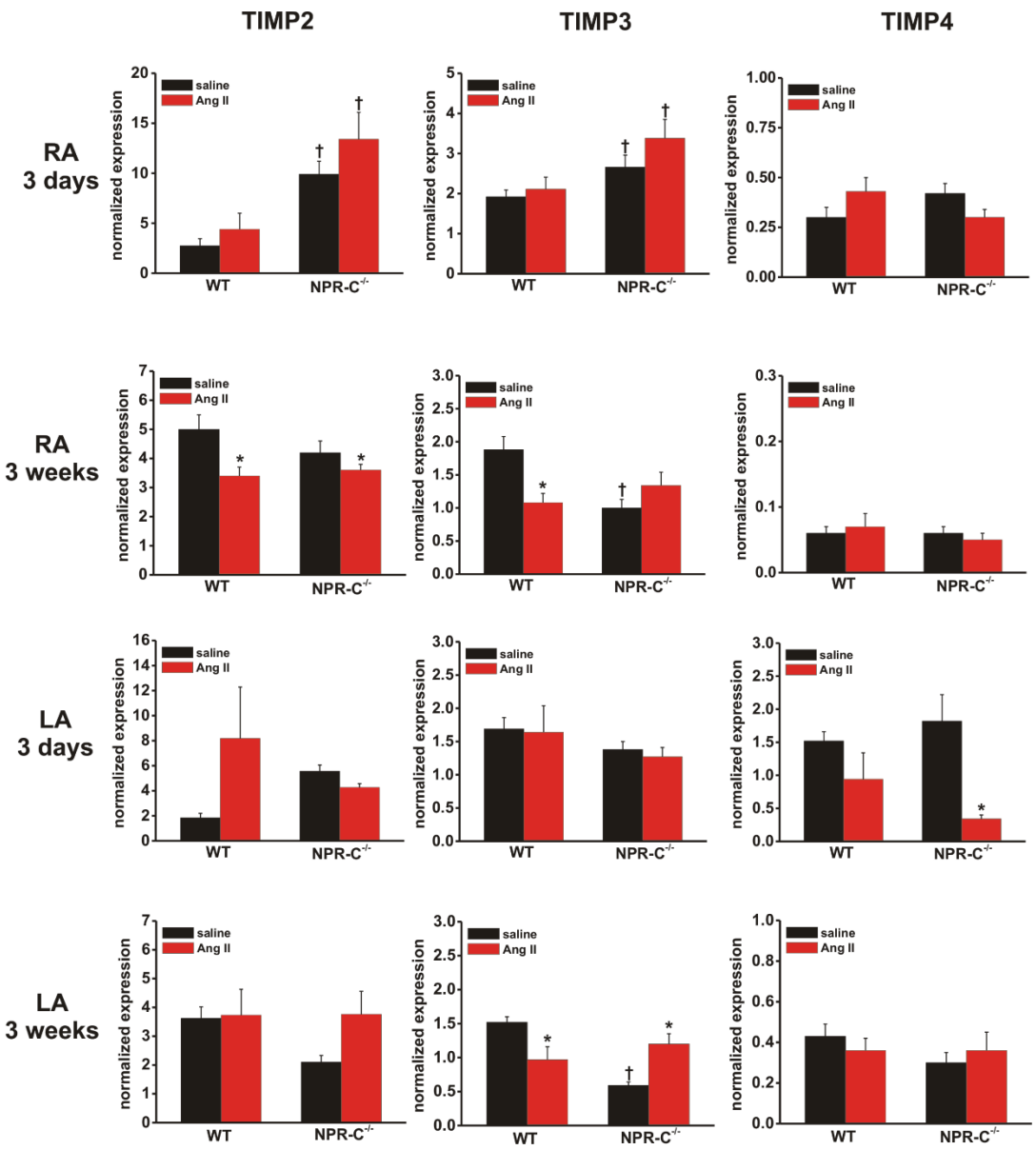

Supplemental Figure 10: Effects of Ang II on TIMP expression in right and left atria from wildtype and NPR-C$^{-/-}$ mice. Summary of mRNA expression for TIMP2, TIMP3 and TIMP4 in the right (RA) and left (LA) after 3 days or 3 weeks of Ang II treatment. **P*<0.05 vs. saline, †*P*<0.05 vs. WT by two-way ANOVA with Tukey's posthoc test; *n*=6 for wildtype/saline, 8 for wildtype/Ang II, 6 for NPR-C$^{-/-}$/saline, 8 for NPR-C$^{-/-}$/Ang II.

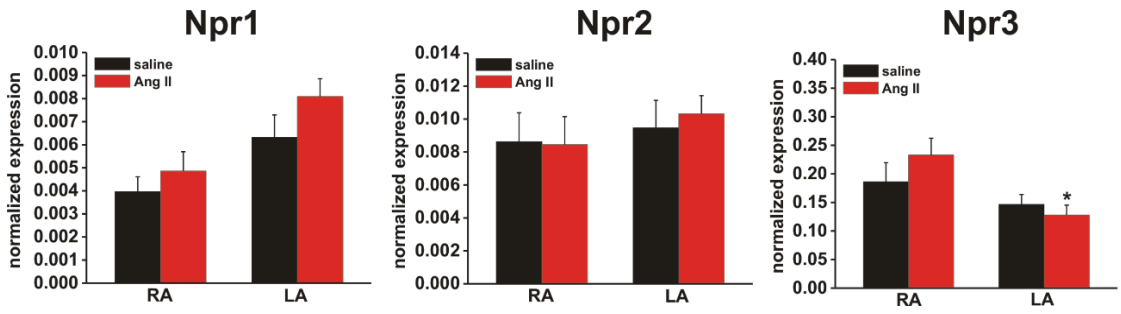

Supplemental Figure 11: Expression of natriuretic peptide receptor genes in the right and left atria in wildtype mice treated with Ang II. Summary of mRNA expression for Npr1 (encodes NPR-A), Npr2 (encodes NPR-B) and Npr3 (encodes NPR-C) in the right (RA) and left (LA) following treatment with saline or Ang II. *P<0.05 vs. RA. Ang II had no effect on expression of Npr1 (P=0.120), Npr2 (P=0.834) or Npr3 (P=0.572). Data analyzed by two-way ANOVA with Tukey's posthoc test; n=7 for RA/saline, 8 for RA/Ang II, 8 for LA/saline and 8 for LA/Ang II.

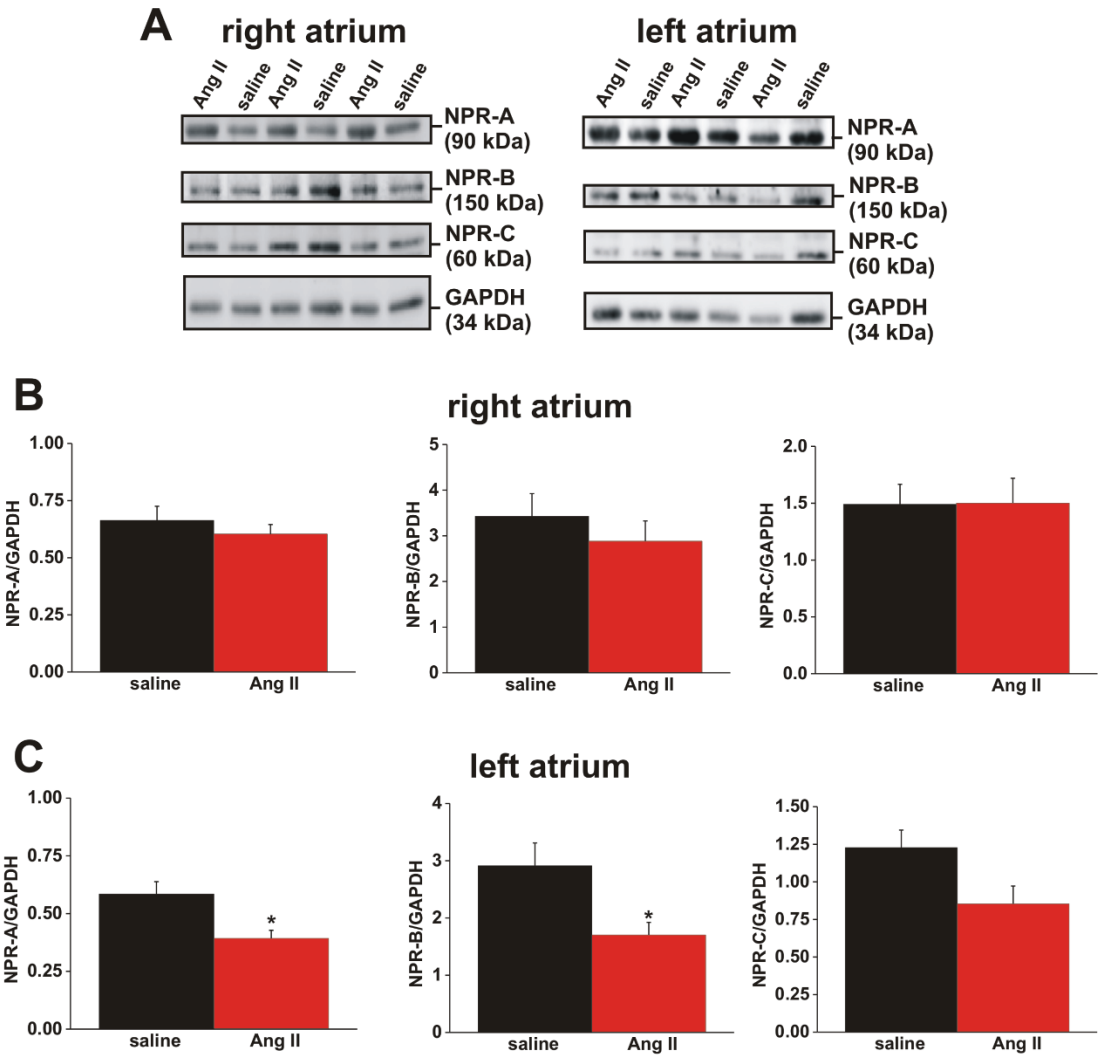

Supplemental figure 12: Expression of natriuretic peptide receptor proteins in the right and left atria in wildtype mice treated with Ang II. A, Representative Western blots for NPR-A, NPR-B and NPR-C protein expression in the right and left atria following saline or Ang II treatment. **B,** Summary data showing no differences in protein expression of NPR-A (*P*=0.446), NPR-B (*P*=0.438) and NPR-C (*P*=0.971) in the right atrium following Ang II treatment. **C,** Summary of the effects of Ang II on protein expression of NPR-A, NPR-B and NPR-C in the left atrium. **P*<0.05 vs. saline; *P*=0.055 for NPR-C in the left atrium. For panels B and C *n*=5 per group. Data analyzed by Student's *t*-test.

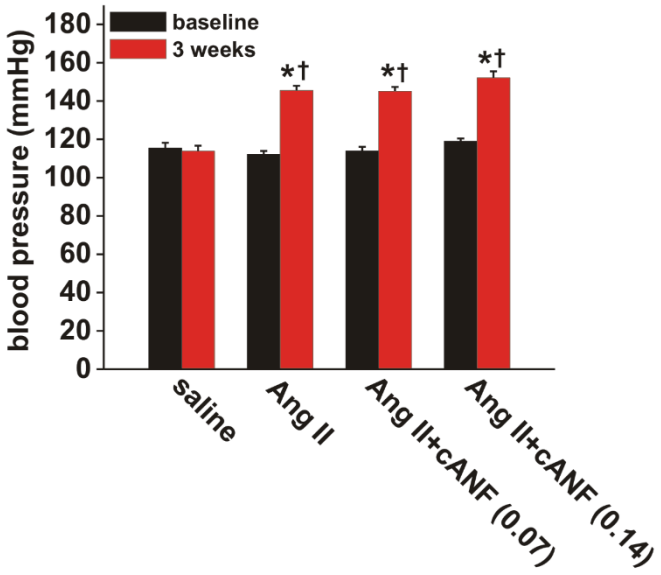

Supplemental Figure 13: Effects of Ang II and cANF on systolic blood pressure in wildtype mice. Measurements were taken at baseline and following three weeks of treatment with saline, Ang II, Ang II + cANF (0.07 mg/kg/day) or Ang II + cANF (0.14 mg/kg/day). *P<0.05 vs. baseline within treatment group, †P<0.05 vs. saline at 3 weeks. There were no differences (P=0.267) in systolic pressure at the 3 week time point between Ang II alone and Ang II + cANF (either dose); n=17 mice for saline, 18 for Ang II, 14 for Ang II + cANF (0.07 mg/kg/day) and 13 for Ang II + cANF (0.14 mg/kg/day).

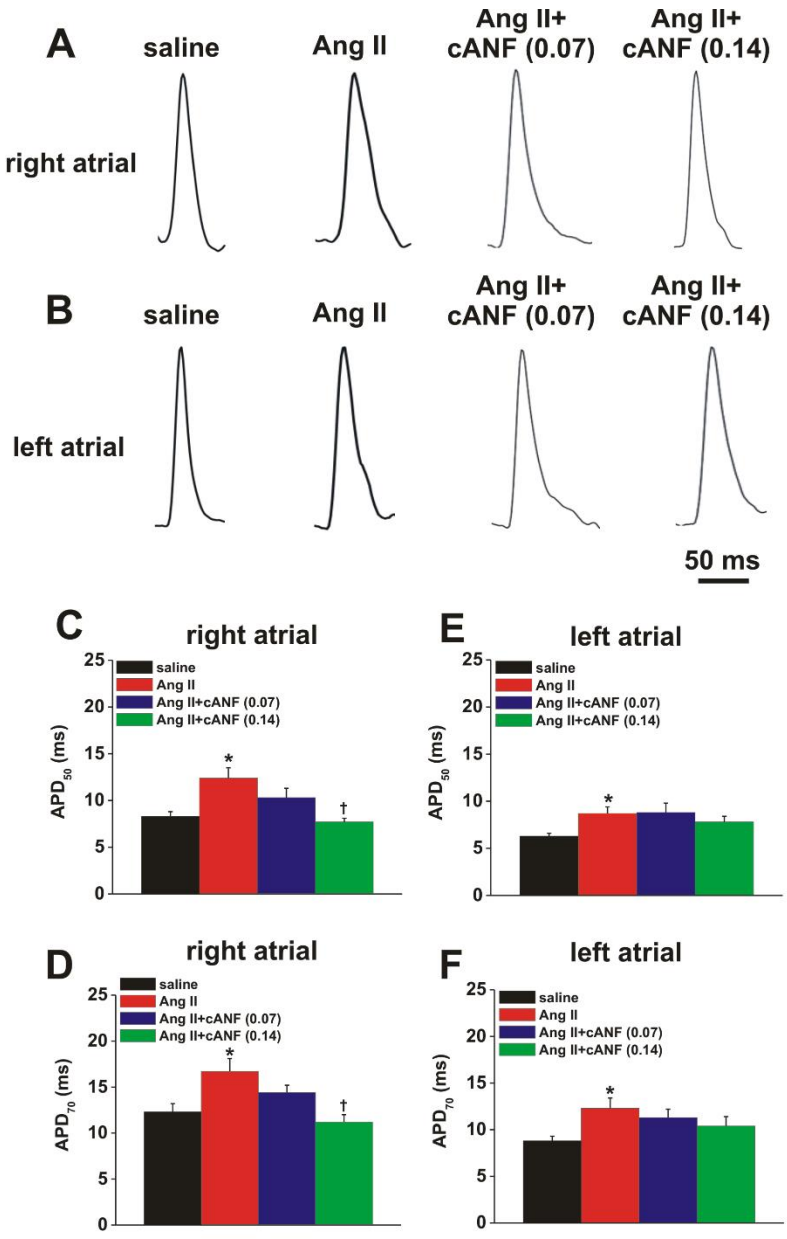

Supplemental Figure 14: Effects of co-treatment with Ang II and cANF on atrial optical action potential duration. A, Representative optical APs in the right atria in wildtype mice treated with saline, Ang II, or Ang II with cANF (0.07 or 0.14 mg/kg/day). **B,** Representative optical APs in the left atria from wildtype mice treated with saline, Ang II or Ang II with cANF (0.07 or 0.14 mg/kg/day). Summary data illustrate the effects of Ang II and cANF on right atrial APD_{50} (**C**) and APD_{70} (**D**) as well as left atrial APD_{50} (**E**) and APD_{70} (**F**). **P*<0.05 vs. saline, †*P*<0.05 vs. Ang II by one-way ANOVA with Tukey's posthoc test; *n*=9 for saline, 9 for Ang II, 7 for Ang II + cANF (0.07) and 8 for Ang II + cANF (0.14).

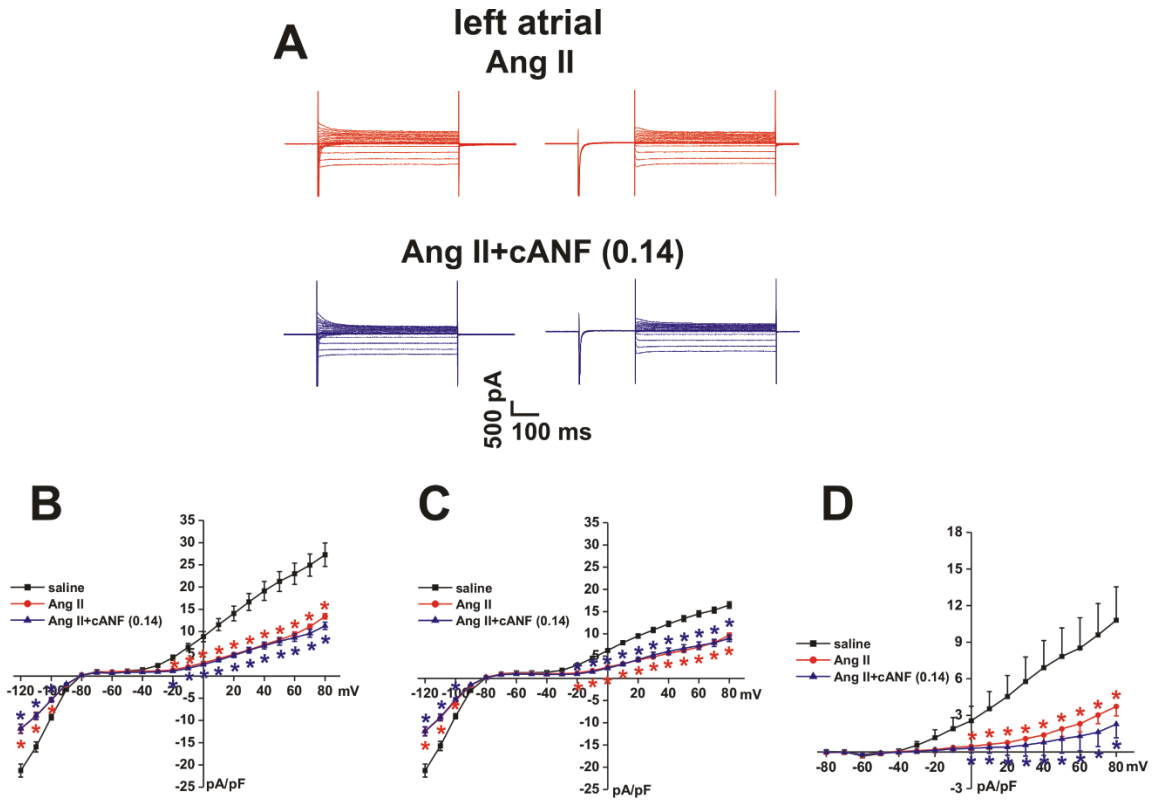

Supplemental Figure 15: Effects of Ang II and cANF on left atrial I_K in wildtype mice. A, Representative I_K recordings with and without an inactivating pre-pulse in left atrial myocytes from mice treated with Ang II alone or Ang II + cANF (0.14 mg/kg/day). **B,** Summary I_K IV curves measured at the peak of the I_K recordings without the pre-pulse in left atrial myocytes from mice treated with saline, Ang II, or Ang II + cANF (0.14 mg/kg/day). **C,** Summary I_K IV curves measured at the peak of the I_K recordings with the pre-pulse in left atrial myocytes from mice treated with saline, Ang II, or Ang II + cANF (0.14 mg/kg/day). **D,** Summary I_{to} IV curves (the difference current between B and C) in left atrial myocytes from mice treated with saline, Ang II, or Ang II + cANF (0.14 mg/kg/day). **P*<0.05 vs. saline by two-way repeated measured ANOVA with Tukey's posthoc test; *n*=12 myocytes for saline, 20 for Ang II and 19 for Ang II + cANF (0.14)

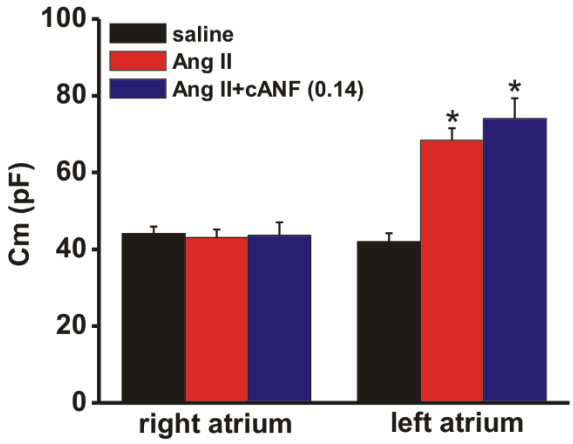

Supplemental Figure 16: Cell capacitance in right and left atrial myocytes from wildtype mice treated with saline, Ang II or Ang II + cANF (0.14 mg/kg/day). **P*<0.05 vs. saline by one-way ANOVA with Tukey's posthoc test within atrial region; for right atrium *n*=29 for saline, 28 for Ang II and 18 for Ang + cANF (0.14); for left atrium *n*=29 for saline, 20 for Ang II and 24 for Ang II + cANF (0.14).

Supplemental Table 1: Duration of arrhythmia in wildtype and NPR-C$^{-/-}$ mice that were induced into atrial fibrillation

	wildtype		**NPR-C$^{-/-}$**	
	saline	**Ang II**	**saline**	**Ang II**
< 5s	100% (2/2)	58% (7/12)	56% (5/9)	47% (7/15)
5-30 s		25% (3/12)	33% (3/9)	27% (4/15)
>30 s		17% (2/12)	11% (1/9)	30% (4/15)

Supplemental Table 2: ECG intervals in wildtype and NPR-C$^{-/-}$ mice treated with Ang II for 3 weeks

	wildtype		**NPR-C$^{-/-}$**	
	saline	**Ang II**	**saline**	**Ang II**
Heart rate (beats/min)	548 ± 6	517 ± 9*	535 ± 10	448 ± 14*†
R-R interval (ms)	109.8 ± 1.2	117.1 ± 2.1*	112.7 ± 2.3	124.7 ± 4.5*†
P wave duration (ms)	25.7 ± 0.5	32.0 ± 0.7*	29.8 ± 0.7	39.6 ± 2.2*†
P-R interval (ms)	43.8 ± 0.7	50.6 ± 0.9*	48.8 ± 0.9	58.9 ± 3.3*†
AERP (ms)	29.1 ± 0.4	35.0 ± 0.9*	33.4 ± 0.7†	39.0 ± 2.1*†
AVERP (ms)	48.6 ± 1.3	56.8 ± 2.2*	52.4 ± 1.2	65.0 ± 2.8*†

Data are means ± SEM; *n* = 23 wildtype/saline, 33 wildtype/Ang II, 14 NPR-C$^{-/-}$/saline, 15 NPR-C$^{-/-}$/Ang II treated mice. *P<0.05 vs. saline within genotype, $^{\dagger}P$<0.05 vs. wildtype within treatment by two-way ANOVA with Tukey's posthoc test.

Supplemental Table 3: Action potential parameters in right atrial myocytes from wildtype and NPR-C$^{-/-}$ mice treated with Ang II for 3 weeks

	wildtype		**NPR-C$^{-/-}$**	
	saline	**Ang II**	**saline**	**Ang II**
RMP (mV)	-78.6 ± 0.5	-78.6 ± 0.6	-77.9 ± 0.5	-76.9 ± 0.7
V_{max} (V/s)	151.2 ± 4.7	146.3 ± 4.9	145.8 ± 7.9	139.7 ± 5.7
OS (mV)	66.1 ± 2.3	63.2 ± 3.1	64.3 ± 2.3	62.1 ± 2.7
APD_{20} (ms)	1.7 ± 0.2	3.9 ± 0.7*	1.5 ± 0.2	3.3 ± 0.4*
APD_{50} (ms)	9.5 ± 1.2	21.5 ± 2.6*	12.0 ± 1.5	23.0 ± 2.5*
APD_{70} (ms)	20.4 ± 2.9	44.2 ± 4.8*	24.9 ± 3.0	48.8 ± 4.7*
APD_{90} (ms)	51.9 ± 5.2	89.7 ± 6.6*	57.2 ± 4.8	107.7 ± 9.7*

RMP, resting membrane potential; V_{max}, AP upstroke velocity; OS, overshoot; APD_{20}, AP duration at 20% repolarization; APD_{50}, AP duration at 50% repolarization; APD_{70}, AP duration at 70% repolarization; APD_{90}, AP duration at 90% repolarization. *P<0.05 vs. saline within genotype by two-way ANOVA with Tukey's posthoc test; n = 18 wildtype/saline, 15 wildtype/Ang II, 23 NPR-C$^{-/-}$/saline, 27 NPR-C$^{-/-}$/Ang II treated right atrial myocytes.

Supplemental Table 4: Action potential parameters in left atrial myocytes from wildtype and NPR-C$^{-/-}$ mice treated with Ang II for 3 weeks

	wildtype		**NPR-C$^{-/-}$**	
	saline	**Ang II**	**saline**	**Ang II**
RMP (mV)	-77.7 ± 0.9	-77.2 ± 1.2	-76.7 ± 0.6	-74.4 ± 0.8†
V_{max} (V/s)	153.9 ± 6.1	121.4 ± 7.3*	141.0 ± 5.2	90.4 ± 6.0*†
OS (mV)	68.4 ± 2.4	53.9 ± 3.1*	61.0 ± 3.4^{+}	43.4 ± 2.4*†
APD_{20} (ms)	1.5 ± 0.1	5.2 ± 1.0*	2.3 ± 0.3	10.4 ± 1.8*†
APD_{50} (ms)	7.5 ± 0.7	28.3 ± 3.8*	9.0 ± 0.9	48.6 ± 8.2*†
APD_{70} (ms)	14.1 ± 1.4	58.4 ± 5.6*	18.3 ± 1.8	89.7 ± 13.2*†
APD_{90} (ms)	41.0 ± 3.5	117.3 ± 7.1*	48.3 ± 3.2	152.4 ± 18.7*†

RMP, resting membrane potential; V_{max}, AP upstroke velocity; OS, overshoot; APD_{20}, AP duration at 20% repolarization; APD_{50}, AP duration at 50% repolarization; APD_{70}, AP duration at 70% repolarization; APD_{90}, AP duration at 90% repolarization. *P<0.05 vs. saline within genotype, $^{\dagger}P$<0.05 vs. wildtype within treatment by two-way ANOVA with Tukey's posthoc test; n = 16 wildtype/saline, 18 wildtype/Ang II, 16 NPR-C$^{-/-}$/saline, 15 NPR-C$^{-/-}$/Ang II treated left atrial myocytes.

Supplemental Table 5: Duration of arrhythmia in wildtype mice treated with Ang II and cANF that were induced into atrial fibrillation

	saline	**Ang II**	**Ang II + cANF (0.07)**	**Ang II + cANF (0.14)**
< 5s 5-30 s >30 s	100% (2/2)	58% (7/12) 25% (3/12) 17% (2/12)	56% (5/9 22% (2/9) 22% (2/9	100% (4/4)

Supplemental Table 6: ECG intervals in wildtype mice co-treated with Ang II and cANF for 3 weeks

	saline	**Ang II**	**Ang II + cANF (0.07)**	**Ang II + cANF (0.14)**
Heart rate (beats/min)	548 ± 6	517 ± 9*	507 ± 9*	549 ± 7†
R-R interval (ms)	109.8 ± 1.2	117.1 ± 2.1*	119.1 ± 2.2*	109.6 ± 1.3†
P wave duration (ms)	25.7 ± 0.5	32.0 ± 0.7*	31.6 ± 0.7*	29.3 ± 0.6*†
P-R interval (ms)	43.8 ± 0.7	50.6 ± 0.9*	49.2 ± 0.9*	46.8 ± 0.9†
AERP (ms)	29.1 ± 0.4	35.0 ± 0.9*	35.9 ± 1.0*	34.5 ± 1.0*
AVERP (ms)	48.6 ± 1.3	56.8 ± 2.2	54.6 ± 2.4	54.5 ± 2.7

Data are means ± SEM; *n* = 23 wildtype/saline, 33 wildtype/Ang II, 20 Ang II with cANF (0.07 mg/kg/day), and 22 Ang II with cANF (0.14 mg/kg/day). **P*<0.05 vs. saline, †*P*<0.05 vs. Ang II by one way ANOVA with Tukey's posthoc test.

Supplemental Table 7: Action potential parameters in right atrial myocytes from wildtype mice co-treated with Ang II and cANF (0.14) for 3 weeks

	saline	Ang II	Ang II + cANF (0.14)
RMP (mV)	-78.6 ± 0.5	-78.6 ± 0.6	-76.6 ± 0.8
V_{max} (V/s)	151.2 ± 4.7	146.3 ± 4.9	140.0 ± 5.6
OS (mV)	66.1 ± 2.3	63.2 ± 3.1	56.0 ± 1.9*
APD_{20} (ms)	1.7 ± 0.2	3.9 ± 0.7*	2.2 ± 0.2†
APD_{50} (ms)	9.5 ± 1.2	21.5 ± 2.6*	12.7 ± 2.3†
APD_{70} (ms)	20.4 ± 2.9	44.2 ± 4.8*	24.5 ± 4.0†
APD_{90} (ms)	51.9 ± 5.2	89.7 ± 6.6*	58.4 ± 6.2†

RMP, resting membrane potential; V_{max}, AP upstroke velocity; OS, overshoot; APD_{20}, AP duration at 20% repolarization; APD_{50}, AP duration at 50% repolarization; APD_{70}, AP duration at 70% repolarization; APD_{90}, AP duration at 90% repolarization. *P<0.05 vs. saline, †P<0.05 vs. Ang II by one way ANOVA with Tukey's posthoc test; n = 18 saline, 15 Ang II, 17 Ang II with cANF (0.14 mg/kg/day).

Supplemental Table 8: Action potential parameters in left atrial myocytes from wildtype mice co-treated with Ang II and cANF (0.14) for 3 weeks

	saline	Ang II	Ang II + cANF (0.14)
RMP (mV)	-77.7 ± 0.9	-77.2 ± 1.2	-77.5 ± 1.0
V_{max} (V/s)	153.9 ± 6.1	121.4 ± 7.3*	116.3 ± 8.5*
OS (mV)	68.4 ± 2.4	53.9 ± 3.1*	48.2 ± 3.0*
APD_{20} (ms)	1.5 ± 0.1	5.2 ± 1.0*	7.1 ± 0.9*
APD_{50} (ms)	7.5 ± 0.7	28.3 ± 3.8*	37.5 ± 5.1*
APD_{70} (ms)	14.1 ± 1.4	58.4 ± 5.6*	74.1 ± 8.8*
APD_{90} (ms)	41.0 ± 3.5	117.3 ± 7.1*	119.4 ± 11.1*

RMP, resting membrane potential; V_{max}, AP upstroke velocity; OS, overshoot; APD_{20}, AP duration at 20% repolarization; APD_{50}, AP duration at 50% repolarization; APD_{70}, AP duration at 70% repolarization; APD_{90}, AP duration at 90% repolarization. *P<0.05 vs. saline by one way ANOVA with Tukey's posthoc test; n = 16 saline, 18 Ang II, 18 Ang II with cANF (0.14 mg/kg/day).

Supplemental Table 9: Quantitative PCR primers

Gene	Gene product	Primer Sequence (5' → 3')	Amplicon length (bp)
Col1a2	Collagen type I	Forward: GCGGACTCTGTTGCTGCTTGC Reverse: GACCTGCGGGACCCCTTTGT	125
Col3a1	Collagen type III	Forward: AGATCCGGGTCCTCCTGGCATTC Reverse: CTGGTCCCGGATAGCCACCCAT	194
TGFβ	TGFβ	Forward: CGAGGTGACCTGGGCACCATCCATGAC Reverse: CTGCTCCACCTTGGGCTTGCGACCCAC	405
TIMP1	TIMP1	Forward: CAGATACCATGATGGCCCCC Reverse: CGCTGGTATAAGGTGGTCTCG	190
TIMP2	TIMP2	Forward: CCAGAAGAAGAGCCTGAACCA Reverse: GTCCATCCAGAGGCACTCATC	112
TIMP3	TIMP3	Forward: GGCCTCAATTACCGCTACCA Reverse: CTGATAGCCAGGGTACCCAAAA	135
TIMP4	TIMP4	Forward: TGCAGAGGGAGAGCCTGAA Reverse: GGTACATGGCACTGCATAGCA	80
Npr1	NPR-A	Forward: CGAAGCTTCCAAGGTGTGACAGG Reverse: GACACAGCCATCAGCTCCTGGG	152
Npr2	NPR-B	Forward: GGGGACTTTCAGCCCGCAGC Reverse: GTGGAGTTTTATCACAGGATGGGTCG	150
Nrp3	NPR-C	Forward: CGAGCGAGTGGTGATCATGTGTG Reverse: CTCCACGAGCCATCTCCGTAGG	147
GAPDH	GAPDH	Forward: AATGGGGTGAGGCCGGTGCT Reverse: CACCCTTCAAGTGGGCCCCG	87
β-actin	β-actin	Forward: CACCCTTCAAGTGGGCCCCG Reverse: CACCCTTCAAGTGGGCCCCG	227

References

1. Egom EE, Vella K, Hua R, Jansen HJ, Moghtadaei M, Polina I, Bogachev O, Hurnik R, Mackasey M, Rafferty S, Ray G, Rose RA. Impaired sinoatrial node function and increased susceptibility to atrial fibrillation in mice lacking natriuretic peptide receptor c. *J Physiol*. 2015;593:1127-1146.
2. Jansen HJ, Moghtadaei M, Mackasey M, Rafferty SA, Bogachev O, Sapp JL, Howlett SE, Rose RA. Atrial structure, function and arrhythmogenesis in aged and frail mice. *Sci Rep*. 2017;7:44336.
3. Azer J, Hua R, Krishnaswamy PS, Rose RA. Effects of natriuretic peptides on electrical conduction in the sinoatrial node and atrial myocardium of the heart. *J Physiol*. 2014;592:1025-1045.
4. Hua R, MacLeod SL, Polina I, Moghtadaei M, Jansen HJ, Bogachev O, O'Blenes SB, Sapp JL, Legare JF, Rose RA. Effects of wild-type and mutant forms of atrial natriuretic peptide on atrial electrophysiology and arrhythmogenesis. *Circ Arrhythm Electrophysiol*. 2015;8:1240-1254.
5. Fedorov VV, Lozinsky IT, Sosunov EA, Anyukhovsky EP, Rosen MR, Balke CW, Efimov IR. Application of blebbistatin as an excitation-contraction uncoupler for electrophysiologic study of rat and rabbit hearts. *Heart Rhythm*. 2007;4:619-626.
6. Farman GP, Tachampa K, Mateja R, Cazorla O, Lacampagne A, de Tombe PP. Blebbistatin: Use as inhibitor of muscle contraction. *Pflugers Arch*. 2008;455:995-1005.
7. Nygren A, Lomax AE, Giles WR. Heterogeneity of action potential durations in isolated mouse left and right atria recorded using voltage-sensitive dye mapping. *Am J Physiol Heart Circ Physiol*. 2004;287:H2634-2643.
8. Morley GE, Vaidya D, Samie FH, Lo C, Delmar M, Jalife J. Characterization of conduction in the ventricles of normal and heterozygous cx43 knockout mice using optical mapping. *J Cardiovasc Electrophysiol*. 1999;10:1361-1375.
9. Jansen HJ, Mackasey M, Moghtadaei M, Belke DD, Egom EE, Tuomi JM, Rafferty SA, Kirkby AW, Rose RA. Distinct patterns of atrial electrical and structural remodeling in angiotensin ii mediated atrial fibrillation. *J Mol Cell Cardiol*. 2018;124:12-25.
10. Springer J, Azer J, Hua R, Robbins C, Adamczyk A, McBoyle S, Bissell MB, Rose RA. The natriuretic peptides bnp and cnp increase heart rate and electrical conduction by stimulating ionic currents in the sinoatrial node and atrial myocardium following activation of guanylyl cyclase-linked natriuretic peptide receptors. *J Mol Cell Cardiol*. 2012;52:1122-1134.
11. Hua R, Adamczyk A, Robbins C, Ray G, Rose RA. Distinct patterns of constitutive phosphodiesterase activity in mouse sinoatrial node and atrial myocardium. *PLoS One*. 2012;7:e47652.
12. Lomax AE, Kondo CS, Giles WR. Comparison of time- and voltage-dependent k+ currents in myocytes from left and right atria of adult mice. *Am J Physiol Heart Circ Physiol*. 2003;285:H1837-1848.
13. Kuo HC, Cheng CF, Clark RB, Lin JJ, Lin JL, Hoshijima M, Nguyen-Tran VT, Gu Y, Ikeda Y, Chu PH, Ross J, Giles WR, Chien KR. A defect in the kv channel-interacting protein 2 (kchip2) gene leads to a complete loss of i(to) and confers susceptibility to ventricular tachycardia. *Cell*. 2001;107:801-813.
14. Fiset C, Clark RB, Larsen TS, Giles WR. A rapidly activating sustained k+ current modulates repolarization and excitation-contraction coupling in adult mouse ventricle. *J Physiol*. 1997;504 (Pt 3):557-563.